Temperature- and Light-Induced Spin Crossover Observed by X-Ray Spectroscopy on Isolated Fe(II) Complexes on Gold

Ben Warner,[⊥†] Jenny C. Oberg,[⊥†] Tobias G. Gill,[⊥‡] Fadi El Hallak,[⊥] Cyrus F. Hirjibehedin,[⊥†‡] Michele Serri,[#] Sandrine Heutz,[#] Marie-Anne Arrio,[&] Philippe Sainctavit,[&] Matteo Mannini,[§] Giordano Poneti,[§¦] Roberta Sessoli[§] and Patrick Rosa[*‖]

⊥ London Centre for Nanotechnology, University College London, London (UK)

† Department of Physics & Astronomy, University College London, London (UK)

‡ Department of Chemistry,University College London, London (UK)

#Department of Materials and London Centre for Nanotechnology, Imperial College London, London (UK)

&Institut de Minéralogie et de Physique des Milieux Condensés, UMR7590, Université Pierre et Marie Curie, Paris (France)

§La.M.M, Department of Chemistry & INSTM Research Unit, Università di Firenze, Florence (Italy)

¦Department of Applied Sciences and Technology, Guglielmo Marconi University, Rome (Italy)

‖ CNRS, Univ. Bordeaux, ICMCB, UPR 9048, F-33600 Pessac, France

Corresponding Author

* CNRS, Univ. Bordeaux, ICMCB, UPR 9048, F-33600 Pessac, France

87 av.Dr. A. Schweitzer, 33608 Pessac Cedex (France)

E-mail: rosa@icmcb-bordeaux.cnrs.fr

ABSTRACT

Using X-ray absorption techniques, we show that temperature- and light-induced spin crossover properties are conserved for a sub-monolayer of the [Fe($H_2B(pz)_2)_2$(2,2'-bipy)] complex evaporated onto a Au(111) surface. For a significant fraction of the molecules, we see changes in the absorption at the $L_{2,3}$ edges that are consistent with those observed in bulk and thick film references. Assignment of these changes to spin crossover is further supported by multiplet calculations to simulate the x-ray absorption spectra. As others have observed in experiments on monolayer coverages, we find that many molecules in our submonolayer system remain pinned in one of the two spin states. Our results clearly demonstrate that temperature- and light-induced spin-crossover is possible for isolated molecules on surfaces, but that interactions with the surface may play a key role in determining when this can occur.

TOC

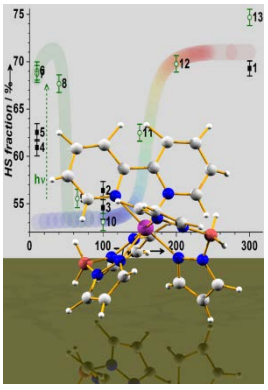

X-ray absorption techniques evidenced that temperature- and light-induced spin crossover properties were conserved for a sub-monolayer of the [Fe($H_2B(pz)_2)_2$(2,2'-bipy)] complex evaporated on a Gold surface

KEYWORDS: spin crossover,·UHV evaporation,·submonolayer,·X-ray absorption,·iron complexes

Spin Crossover (SCO) complexes are promising building blocks for spintronic[1] and high-density memory devices because they contain a d^4 to d^7 transition metal ion that can be reversibly switched between two distinct spin states, Low-Spin (LS) and High-Spin (HS).[2-3] This phenomenon can be driven using a variety of external inputs, including temperature,[4-5] light,[6-8] pressure,[9] magnetic field,[10] mechanical stress[11] and charge flow.[12-17] Recently, there has been a surge of interest in the study of the conversion properties of nanostructured SCO materials, in the form of nanoparticles,[18-22] thick films,[23-25] and even isolated molecules either bridging nanogaps[13-15] or on surfaces.[16-17] Integration of switchable molecular materials in nanoscale devices requires the retention of their conversion properties once deposited on a solid substrate. SCO systems are known to display conversion features hugely dependent on the environment, and can be easily perturbed by the molecule's interaction with the surface. Recently clean Ultra High Vacuum (UHV) deposition of thermally evaporable SCO molecules has allowed preparing submonolayer deposits. By using Scanning Tunneling Microscopy (STM) it has been shown that SCO molecules, decoupled from underlying metallic surfaces, either by another layer of molecules[12] or by a thin insulator[16] such as CuN,[26] exhibit voltage-induced switching. However, electrically-induced switching of SCO molecules placed directly on metal surfaces was not possible,[12,16] though the coexistence of molecules pinned in the HS and LS states has been observed using low-temperature X-ray Absorption Spectroscopy (XAS) and X-ray Magnetic Circular Dichroism (XMCD).[16] In addition, while temperature driven SCO has been detected for a different Fe^{II} complex evaporated on HOPG (Highly Ordered Pyrolytic Graphite),[27] evidence of light-induced spin state switching for surface confined SCO molecules is still lacking.

Here we report the detection of temperature- and light-induced SCO for isolated molecules of complex $[Fe(H_2B(pz)_2)_2(bipy)]$ **1** (Scheme 1) on Au(111), using X-ray absorption

techniques along with multiplet calculations. Such results, which have not yet been reported, offer direct evidence that temperature- and light-induced SCO, in addition to electrically induced switching,[16] is indeed possible for isolated molecules even on metallic substrates. In the bulk, SCO behavior is quite sensitive to the molecules' environment, and our results suggest that for sub-monolayers both interactions with the surface and neighboring molecules may play a role in inhibiting the SCO phenomenon.

Scheme 1.

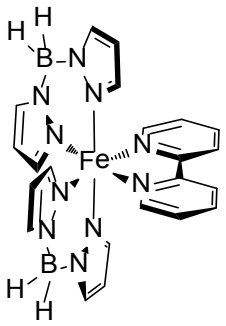

1

In order to detect thermally and light-driven SCO, XAS was employed,as done previously on the model SCO complex $[Fe(NCS)_2(phen)_2]$ in the bulk phase,[28-30] due to the technique's element, oxidation, and spin state selectiveness. Most importantly, the extreme sensitivity afforded by the Total Electron Yield (TEY) detection of X-Ray absorption[31-36] allows for the investigation of submonolayer deposits, as recently reported for Fe^{II} based SCO complexes sublimed on CuN@Cu[16] and HOPG[27].

Using variable temperature X-ray absorption spectra, we examined a submonolayer coverage evaporated *in situ* under UHV conditions on Au(111), before and after irradiation with visible laser light. We compare these results to those obtained from two other samples: 1) a

single crystal finely scratched on gold foil, which we use as a spectroscopic bulk reference; and 2) a 300 nm thick film sublimed*ex situ* on copper foil, to check the preservation of structure and properties of the complex. Experimental spectra were then compared to the ones obtained using multiplet calculations.[37-39]

The variation of the $L_{2,3}$ edge spectra for the bulk sample over the range of the thermal spin crossover (100-300 K) is reported in Figure 1a(see also Figure S1 in Supplementary Information). Both L_2 (721.5 to 721.9 eV) and L_3 maxima (708.7 to 710.0 eV) shift to higher energies when temperature is decreased, with aL_2 edge less structured and more intense under 150 K. The branching ratio,[40-41] defined as $I_3/(I_3+I_2)$ where I stands for the integrated intensity at the corresponding L edge, decreases from 0.78 at 300 K to 0.64 at 100 K. As observed for complex $[Fe(NCS)_2(phen)_2]$,[28-30]and recently for a monolayer of another complex $[Fe(NCS)_2L]$,[28] all these features are associated with the reversible transition from a $t_{2g}^4e_g^2$ configuration (S=2) at 300 K to $t_{2g}^6e_g^0$ (S=0) at low temperature. These results are in good agreement with previous X-ray photoemission data.[42]Spectra measured at 300 K before and after the temperature cycle are identical, confirming that the SCO process is fully reversible with no X-ray induced degradation.

Experimental spectra at 300 K and 100 K show in both cases excellent agreement with spectra resulting from the ligand field multiplet calculations,[43] with an O_h crystal field parameter $10Dq$ of 1 eV for the HS configuration and 2.2 eV for the LS one. These are similar to values reported for complex $[Fe(NCS)_2(phen)_2]$: respectively 0.5 and 2.2 eV,[37] or 0.9 and 2.2 eV.[30] These $10Dq$ values can be compared with the range predicted for the occurrence of SCO from ligand field theoretical considerations: $10D_q^{HS} \approx 1.36\text{-}1.55$ eV and $10D_q^{LS} \approx 2.36\text{-}2.73$ eV.[2b] The

discrepancy for $10D_q^{HS}$ has been explained by the fact that XAS is only sensitive to the excited state crystal field splitting for high-spin complexes.[37]

a)

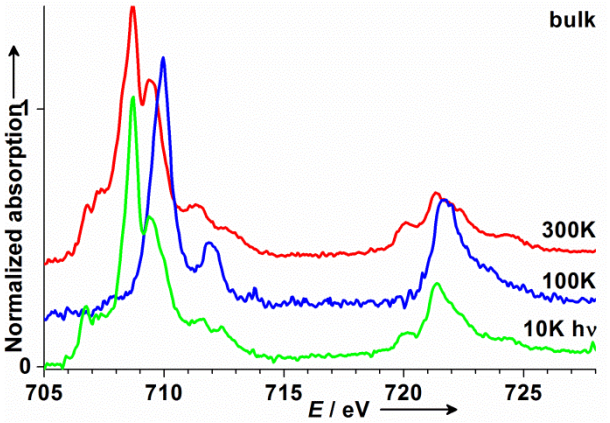

b)

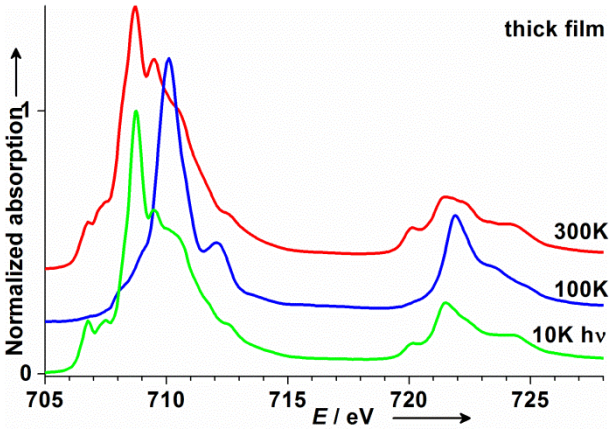

c)

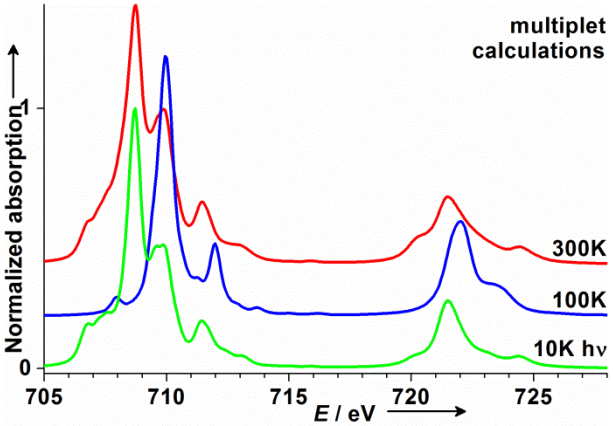

Figure 1. Normalized spectra of **1** (absorption maximum) at 300 K (red line), 100 K (blue line)and 10 K (green line) after illumination (658 nm *cw* laser, 15 $mW.cm^{-2}$) for (a) the bulk and (b) the 300 nm thick film with (c) the corresponding calculated spectra. Spectra are shifted vertically for clarity.

Spectra measured on the thick film prepared *ex situ* are similar to the bulk, and show comparable temperature dependence (Figure 1b and Figure S1). Nevertheless, the thick film spectrum is slightly differentfrom the bulk compound: shoulders on the high-energy side (at 300 K) or at the low-energy side (at 100 K) of the L_3 absorption peak, are likely associated with a small fraction of decomposition product, which maybe caused by air exposure of this sample prepared *ex situ*.The analysis of the temperature-dependent spectra as weighted sums of the bulk spectra at 300 K and 100 K, chosen as representative of the HS and LS state respectively, allows for the extraction of the temperature dependence of the HS fraction (Table S2). For the thick film, the shoulder signals were found to be temperature independent, and thus do not affect the switching behavior. We extracted this spurious contribution (Figures S3 and S4) and subtracted it from all spectra before evaluating the HS fraction (Table S5). Figure 2summarizes the result of these analyses, together with the HS fraction derived from magnetometricinvestigations.[44]The agreement between experimental data obtained with different techniques is excellent.

Spectra of the bulk and the thick film at 10 K after laser irradiation, with the corresponding spectrum resulting from multiplet calculations, are also shown in Figure 1. Before irradiation, in the dark, the bulk is almost completely in the LS state, though for the thick film a more significant HS component is detected (Figure 2). This is the result of some spin conversion resulting from X-ray irradiation, the SOft X-ray Induced Excited Spin State Trapping (SOXIESST) already reported on $[Fe(NCS)_2(phen)_2]$,[29] as well as for different switchable

molecular species.[45]The effect is already visible at 50 K; however we do not observe the irreversible X-ray induced photoconversion that was reported for $[Fe(NCS)_2(phen)_2]$.[29] As already seen by photomagnetic measurements on a thick film of compound **1** on Kapton,[25] the film at 10 K is more sensitive to photons, here at X-ray wavelengths, than the bulk.

cw laser irradiation at 10 K (658 nm, 15 $mW.cm^{-2}$) readily populates the HS state by the LIESST effect (Light-Induced Excited Spin State Trapping).[7-8,46]After switching off laser irradiation, the relaxation of the HS trapped state could be followed with increasing temperature (see Figure S6), yielding the fraction of the metastable HS statereported in Figure 2.

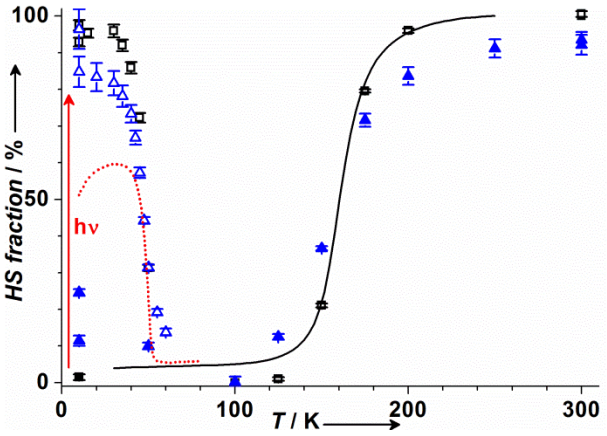

Figure 2.HS fraction *vs.* temperature derived from the linear interpolation of the XAS spectra for the bulk compound before (filled black squares) and after illumination (empty black squares), and the 300 nm thick film before (filled blue triangles) and after illumination (empty blue triangles), compared to the magnetometricresults on the bulk compound before (full line) and after illumination (red dotted line).

The efficiency of the light-induced conversion is close to 100%, as compared to some 60-80% as determined by magnetic measurements. This is not surprising since, asin reflectometry measurements,[25] TEY is probing the topmost layers of the sample (typically 1-5 nm),[47-49] a

thickness much smaller than the light penetration depth. The relaxation behavior of the film and the bulk is similar to what is observed with reflectometry or photomagnetic measurements, with similar T_{LIESST} temperatures.[50]

The evaluation of the magnetic response through XMCD spectra fully supports our assignment of HS and LS states. Compound **1** behaves as a paramagnet: the XMCD signal measured is weak at 300 K, increases until SCO occurs, then becomes very weak down to 10 K. It increases again with photoexcitation at low temperatures, with spectra corresponding quite well with the calculated spectrum, and then decreases with temperature induced relaxation (Figures S7 to S9).[51]

With the experimental method fully established on the bulk and the evaporated thick film, we moved to a sub-monolayer coverage sample grown on Au(111), which we prepared *in situ* at the ID08 ESRF beamline. XAS spectra allowed us to evaluate the amount of molecules sublimed onto the Au surface by measuring theFe edge jump (*i.e*. the ratio of intensities before and after the L_3 edge),[52-53]provided that absorption for ions other than the Fe atoms of the molecule is negligible compared to the Au(111) substrate absorption, which is a valid assumption here. We found anedge jump of 2.3%,which is lower than the ones reported for another Fe(III)-based molecular system prepared by monolayer self-assembly[36],and for 0.8 monolayers of another SCO complex on HOPG.[27] As detailed in Figure S11 in Supporting Information, this edge jump, being 100 times smaller than the ones found for the bulk and thick film samples, gives an approximate coverage about 0.03 to 0.14 monolayers, thus allowing to safely exclude the presence of multilayer islands that would moreover be clearly visible on STM images.[54]

Figure 3 reports for this sample the evolution of XAS spectra between 100 K and 300 K. The analysis of the spectra in Fig. 3a(relative ratio of peaks at 708.7 and 710.0 eV) points out that even at 300 K we have a mixture of molecules in both spin states, as also reported previously for a related SCO complex.[12] When lowering the temperature from 300 K to 100 K the change of this ratio as well as the increase of the intensity of the L_2 peak show clearly that the HS/LS ratio decreases, according to the expected SCO behavior, although these changes are not as large as they are in the bulk or thick film samples. This clear non-monotonic temperature dependence of XAS excludes spurious temperature-induced changes such as sample damage under the beam, or ice deposition on the sample.Thus thermal spin crossover is clearly observed but only for a fraction of the molecules covering the surface. The remainder is trapped in either the LS or the HS state, showing that for some molecules the electronic state and/or the geometry are affected by the surface. As detailed in Figure 3b and 3c, spectra are excellently reproduced by a linear combination of the HS and LS spectra of the bulk compound,showing that we obtained intact molecules of compound **1**.

a)

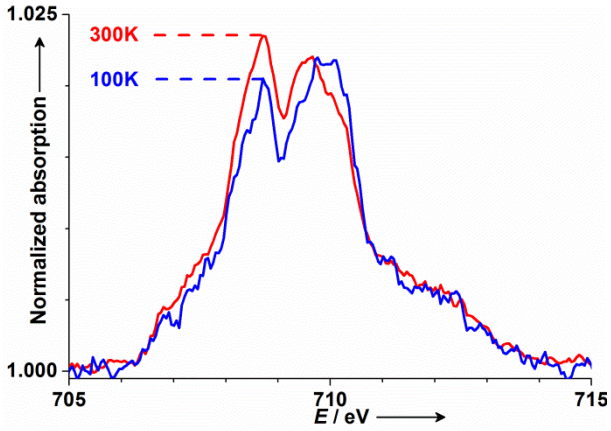

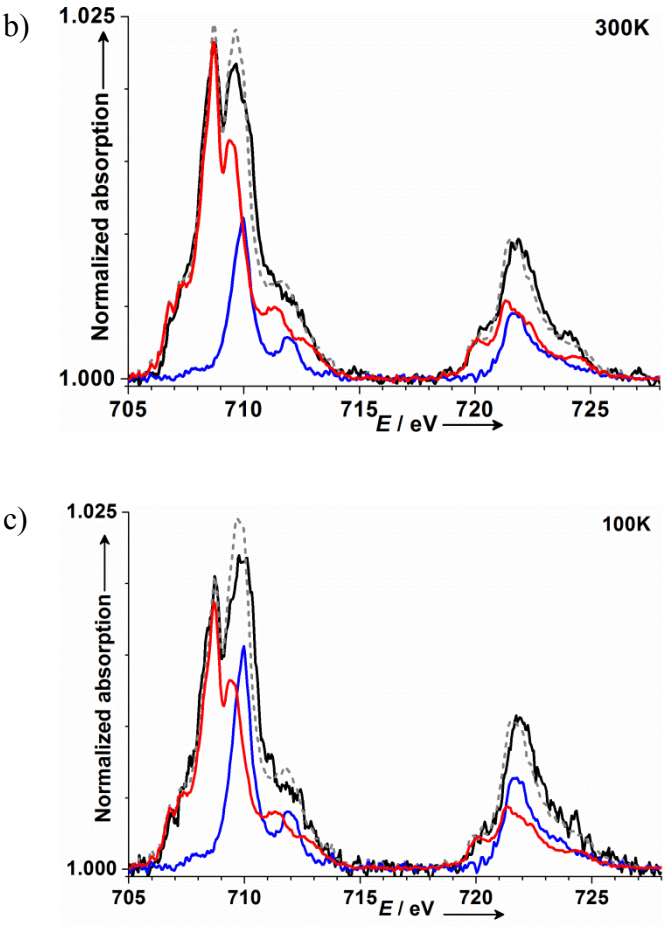

Figure 3. a) Comparison of spectra at the L_3edge (705-715 eV) for the sub-monolayer sample of **1**at 300 Kand 100 K (red and blue lines respectively); b) T=300K, experimental spectrum (black line) , with corresponding HS (red line) and LS (blue line) components, and linear combinations (dashed grey line) for HS/LS ratios of 69:31 at 300 K;c)T=100K, experimental spectrum (black line) with corresponding HS (red line) and LS (blue line) components, and linear combinations (dashed grey line) for HS/LS ratios of 56:44 at 100 K. Spectra were normalized at 705eV (see Table S13for more details).

Figure 4 reports for this sample the evolution of XAS spectra at 10 K after irradiation with visible light, compared to the spectrumat 100 K. The spectrum at 10 K (see Table S13) before irradiation as compared to the earlier spectrum at 100 K shows an increase of the HS

fraction, caused by the SOXIESST effect already seen for the bulk. When irradiatingwith visible light (*cw* laser, 658nm, 15min),the effect is also in this case larger than the SOXIESST effect, bringing the LS/HS ratio back to values observed at room-temperature. The behavior of the changes in the spectra with light exposure, and the reversal of these changes upon increasing the temperature after irradiation further support our assignment of this phenomenon to spin crossover.

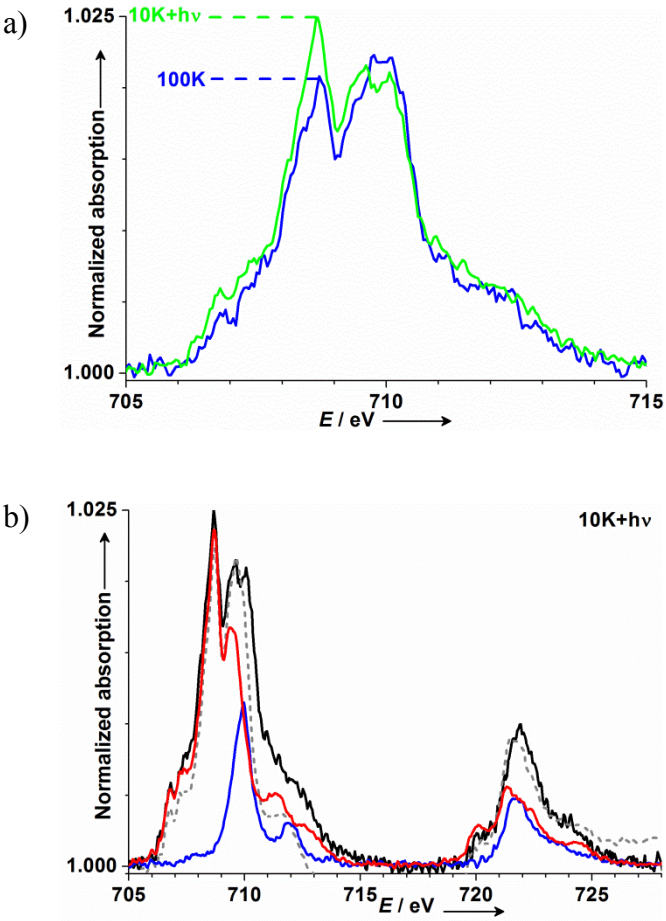

Figure 4. a) Comparison of spectra at the Fe L_3edge (705-715 eV) for the sub-monolayer sample of **1** at 100 K then at 10 K after laser irradiation (658 nm *cw* laser, 15 mW.cm^{-2}) (blue and green lines respectively). b)Experimental spectra at 10 K after irradiation (black line), with corresponding HS (red line) and LS (blue line) components, and the linear combination for a

HS/LS ratio of 69:31 (dashed grey line). Spectra were normalized at 705eV (see Table S13for more details).

We applied the same procedure previously employed for the bulk sample and thick film to quantify this HS molar fraction in the submonolayer. Figure 5 and Table S13, reporting the evolution with temperature of the HS fraction of the sub-monolayer, evidence a transition profile in excellent agreement with the ones previously found. Error bars on individual points are smaller than the observed variations with temperature and light irradiation, thus excluding any fit bias.

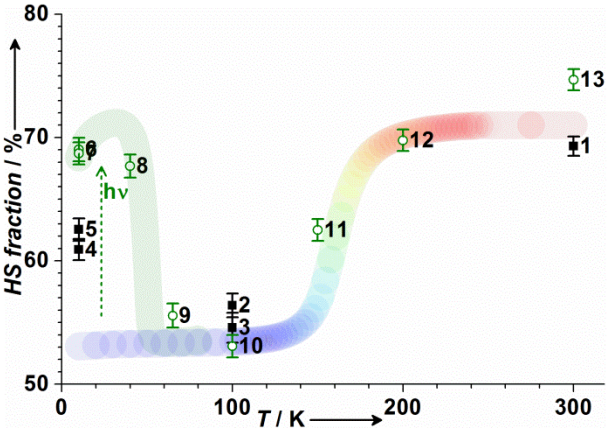

Figure 5.HS fraction *vs.* temperature derived from the linear interpolation of the XAS spectra for the sub-monolayer sample: filled squares are before laser irradiation, green empty circles are after laser irradiation (numbers label the acquisition order).As a guide to the eye the shifted and rescaled temperature dependence of the thermal- and photo-induced high spin fractions of the bulk specimen are drawn as faded bands. Note that the HS fraction scale ranges from 50 to 80% for clarity.

From this analysis we observe that 20% of the moleculesshow a SCO behavior similar to the one observed on the bulk or the thick film, whilethe remaining molecules are trapped in a definite spin state: 53(1)% in HS, and 27(2)% in LS.

Although only a fraction of the deposited molecules exhibits SCO behaviorit has been possible to characterize in detail their conversion process. In particular they have revealed:

(i) thermal SCO with a transition temperature around 160 K, similar to the one observed for the bulk, an indirect piece of evidence that we have intact molecules on the surface, but with a seeminglysmoother temperature dependence, as observed on highly diluted SCO systems;[55]

(ii) SOXIESST at low temperature in the dark causing a partial conversion to the HS state of the switchable molecules;

(iii) a quick and full conversion of the remaining molecules to the HS state upon *cw* laser irradiation at 658 nm;

(iv) complete relaxation of the metastable photoinduced state to the LS state between 40 and 65 K, comparable with the bulk phase where T_{LIESST} = 52 K. This is expected if the molecule has preserved its structure on the surface, since this relaxation behavior was shown to depend primarily on the first coordination sphere of the metal ion;[56]

(v) a reversible transformation, with two 300 K spectra measured before and after thermal- and light-induced SCO showing close HS/LS proportions.

In summary, we have observed thermal- and light-induced SCO on sub-monolayer coverage of complex **1** on Au(111).The transition appears to be fully reversible, and its features

are virtually identical to the ones observed on the bulk. This demonstrates that spin crossover complexes retain their properties at the single molecule level even on metallic substrates, which allows for the possibility of addressing their spin states through temperature or light in spintronic applications,[57]while electrical switching can also be envisaged. We observedhowever also a mixture of HS and LS pinned states throughout the full temperature range for our submonolayer coverage. This suggests a certain sensitivity of the switchable behavior of SCO to the environment. In fact switching was not observed for a full monolayer of complex **1** on Au(111),[12]and of complex $[Fe(NCS)_2(phen)_2]$ on Cu(100),[16] but was observed for a monolayer on HOPG of complex $[Fe(NCS)_2L]$.[27] The latter complex shows a much more gradual SCO, hinting that cooperative interactions between the molecules may play a role in blocking SCO. Future theoretical and experimental studies, particularly with probes that can determine the precise binding configuration of the molecules on a given surface for various coverages, may shed more light on the reasons why some molecules remain trapped while others undergo spin crossover. The observation that the spin state can be switched by light also in the case of molecules deposited on a conducting substrate increases significantly the interest in SCO molecules as potential building blocks for single molecule devices.

Author Contributions

The manuscript was written through contributions of all authors. All authors have given approval to the final version of the manuscript.

Funding Sources

Funding from ANR-11-JS07-013-01-CHIROTS, Région Aquitaine (P.R), EPSRC Grants EP/D063604/1, EP/H002367/1 (B.W., J.C.O., T.G., F.E.H, C.F.H.), E.P/H002022/1 (M.S, S.H), EP/F04139X/1 (S.H.), ERC Advanced Grant MolNanoMaS proj. n. 267746 (M.M, G.P., R.S) and NanoPlasMag proj. RBFR10OAI0 (M.M.).

ACKNOWLEDGMENT

We acknowledge ESRF for providing beam time under projects HE3523 and HE3754 and we thank Julio Cezar Criginski, Flora Yakhou and Kurt Kummer for their help during beamtime. We also thank Joris van Slageren for stimulating discussions.

Supporting Information Available.Full experimental details, bulk and thin film XAS spectra variation with temperature (Figure S1, S3, S4), deconvolution results for the bulk (Table S2) and the thick film (Table S5), relaxation of the photoinduced HS state for the bulk monitored by XAS (Figure S6), XMCD spectra for the thick film (Figure S7) and the bulk (Figure S8), comparison of XAS/XMCD spectra with multiplet calculations (Figure S9), XAS/XMCD spectra of the spurious component (Figure S10), unscaled XAS spectra at 300 K for all samples (Figure S11), STM images of the submonolayer sample (Figure S12), deconvolution results for the submonolayer (Table S13). This material is available free of charge viathe Internet at http://pubs.acs.org.

REFERENCES

[1] Schmaus, S.; Bagrets, A.; Nahas, Y.; Yamada, T. K.; Bork, A.; Bowen, M.; Beaurepaire, E.; Evers, F.; Wulfhekel,W. Giant magnetoresistance through a single molecule, *Nature Nanotech.***2011**, *6*, 185-189.

[2] Gütlich, P.; Goodwin, H. A. Spin Crossover-An Overall Perspective.*Top.Curr. Chem.***2004**, *233*, 1-48.

[3] Hauser, A. Ligand Field Theoretical Considerations. *Top.Curr. Chem.***2004**, *233*, 49-58.

[4] Gütlich, P.; Hauser, A.; Spiering, H. Thermal and Optical Switching of Iron(II) Complexes. *Angew. Chem. Int. Ed. Engl.***1994**, *33*, 2024-2054.

[5] Gütlich, P.; Garcia, Y.; Goodwin, H. A. Spin crossover phenomena in Fe(II) complexes. *Chem. Soc. Rev.***2000**, *29*, 419-427.

[6] Gütlich, P.; Garcia, Y.; Woike, T. Photoswitchable coordination compounds. *Coord. Chem. Rev.***2001**, *219-221*, 839-879.

[7] Hauser, A. Light-Induced Spin Crossover and the High-Spin→Low-Spin Relaxation. *Top.Curr. Chem.***2004**, *234*, 155-198.

[8] Hauser, A.; Enachescu, C.; Lawson Daku, M.; Vargas, A.; Amstutz, N. Low-temperature lifetimes of metastable high-spin states in spin-crossover and in low-spin iron(II) compounds: The rule and exceptions to the rule. *Coord. Chem. Rev.***2006**, *250*, 1642-1652.

[9] Ksenofontov, V.; Gaspar, A. B.; Gütlich, P. Pressure Effect Studies on Spin Crossover and Valence Tautomeric Systems. *Top.Curr. Chem.***2004**, *235*, 23-64.

[10] Bousseksou, A.; Varret, F.; Goiran, M.; Boukheddaden, K.; Tuchagues, J.-P. The Spin Crossover Phenomenon Under High Magnetic Field.*Top.Curr. Chem.***2004**, *235*, 65-84.

[11] Parks, J. J.; Champagne, A. R.; Costi, T. A.; Shum, W. W.; Pasupathy, A. N.; Neuscamman, E.; Flores-Torres, S.; Cornaglia, P. S.; Aligia, A. A.; Balseiro, C. A.;*et al.* Mechanical Control of

Spin States in Spin-1 Molecules and the Underscreened Kondo Effect.*Science***2010**, *328*, 1370-1373.

[12] Gopakumar, T. G.; Matino, F.; Naggert, H.; Bannwarth, A.; Tuczek, F.; Berndt, R. Electron-Induced Spin Crossover of Single Molecules in a Bilayer on Gold.*Angew. Chem. Int. Ed.***2012**, *51*, 6262-6266.

[13] Meded, V.; Bagrets, A.; Fink, K.; Chandrasekar, R.; Ruben, M.; Evers, F.; Bernand-Mantel, A.; Seldenthuis, J. S.; Beukman, A.; van der Zant, H. S. Electrical control over the Fe(II) spin crossover in a single molecule: Theory and experiment. *Phys. Rev. B*, **2011**, *83*, 245415 1-13.

[14] Aravena, D.; Ruiz, E. Coherent Transport through Spin-Crossover Single Molecules. *J. Am. Chem. Soc.***2012**, *134*, 777−779.

[15] Prins, F.; Monrabal-Capilla, M.; Osorio, E. A.; Coronado, E.; van der Zant, H. S. J. Room-Temperature Electrical Addressing of a Bistable Spin-Crossover Molecular System.*Adv. Mater.***2011**, *23*, 1545-1549.

[16] Miyamachi, T.; Gruber, M.; Davesne, V.; Bowen, M.; Boukari, S.; Joly, L.; Scheurer, F.; Rogez, G.; Yamada, T. K.; Ohresser, P.; *et al.*Robust spin crossover and memristance across a single molecule.*Nature Commun.*,**2012**, *3*, 938:1-6.

[17] Alam, M. S.; Stocker, M.; Gieb, K.; Müller, P.; Haryono, M.; Student, K.; Grohmann, A. Spin-State Patterns in Surface-Grafted Beads of Iron(II) Complexes. *Angew.Chem. Int. Ed.***2010**, *49*, 1159 –1163.

[18] Létard, J.-F.; Daro, N.; Nguyen, O. Nanoparticles of a spin transition compound.*Patent* WO 2007/065996 (2007-06-14).

[19] Volatron, F.; Catala, L.; Rivière, E.; Gloter, A.; Stéphan, O.; Mallah, T. Spin-Crossover Coordination Nanoparticles. *Inorg. Chem.*, **2008**, *47*, 6584.

[20] Larionova, J.; Salmon, L.; Guari, Y.; Tokarev, A.; Molvinger, K.; Molnár, G.; Bousseksou, A. Towards the Ultimate Size Limit of the Memory Effect in Spin-Crossover Solids.*Angew. Chem. Int. Ed.*,**2008**,*47*, 8236-8240.

[21] Forestier, T.; Kaiba, A.; Pechev, S.; Denux, D.; Guionneau, P.; Etrillard, C.; Daro, N.; Freysz, E.; Létard,J.-F. Nanoparticles of $[Fe(NH_2\text{-}trz)_3]Br_2$-3 H2O ($NH_2$-trz=2-Amino-1,2,4-triazole) Prepared by the Reverse Micelle Technique: Influence of Particle and Coherent Domain Sizes on Spin-Crossover Properties*Chem. Eur. J.*, **2009**, *15*, 6122-6130.

[22] Galan-Mascaros, J. R.; Coronado, E.; Forment-Aliaga, A.; Monrabal-Capilla, M.; Pinilla-Cienfuegos, E.; Ceolin, Marcelo, M. Tuning Size and Thermal Hysteresis in Bistable Spin Crossover Nanoparticles.*Inorg. Chem.***2010**, *49*, 5706-5714.

[23] Mahfoud, T.; Molnár, G.; Cobo, S.; Salmon, L.; Thibault, C.; Vieu, C.; Demont, P.; Bousseksou, A. Electrical properties and non-volatile memory effect of the $[Fe(HB(pz)_3)_2]$ spin crossover complex integrated in a microelectrode device. *Appl. Phys. Lett.***2011**, *99*, 053307 1-3.

[24] Shi, S.; Schmerber, G.; Arabski, J.; Beaufrand, J.-B.; Kim, D. J.; Boukari, S.; Bowen, M.; Kemp, N. T.; Viart, N.; Rogez, G.;*et al.* Study of molecular spin-crossover complex $Fe(phen)_2(NCS)_2$ thin films.*Appl. Phys. Lett.***2009**, *95*, 043303 1-3.

[25] Palamarciuc, T.; Oberg, J. C.; El Hallak, F.; Hirjibehedin, C. F.; Serri, M.; Heutz, S.; Létard, J.-F.; Rosa, P. Spin crossover materials evaporated under clean high vacuum and ultra-high vacuum conditions: from thin films to single molecules. *J. Mater. Chem.***2012**, *22*, 9690-9695.

[26] Hirjibehedin, C. F.; Lutz, C.; Heinrich, A. Spin Coupling in Engineered Atomic Structures.*Science***2006**, *312*, 1021–1024.

[27] Bernien, M.; Wiedemann, D.; Hermanns, C. F.; Krüger, A.; Rolf, D.; Kroener, W.; Müller, P.; Grohmann, A.; Kuch, W. Spin Crossover in a Vacuum-Deposited Submonolayer of a Molecular Iron(II) Complex. *J. Phys. Chem. Lett.*, **2012**, *3*, 3431-3434.

[28] Cartier dit Moulin, C.; Rudolf, P.; Flank, A.-M.; Chen, C.-T. Spin Transition Evidenced by Soft X-ray Absorption Spectroscopy. *J. Phys. Chem.***1992**, *96*, 6196-6198

[29] Collison, D.; Garner, C. D.; McGrath, C. M.; Mosselmans, J. F. W.; Roper, M. D.; Seddon, J. M. W.; Sinn, E.; Young, N. A.Soft X-ray induced excited spin state trapping and soft X-ray photochemistry at the iron $L_{2,3}$ edge in $[Fe(phen)_2(NCS)_2]$ and $[Fe(phen)_2(NCSe)_2]$ (phen = 1,10-phenanthroline)*J. Chem. Soc., Dalton Trans.***1997**, 4371-4376.

[30]Lee, J.-J.; Sheu, H.; Lee, C.-R.; Chen, J.-M.; Lee, J.-F.; Wang, C.-C.; Huang, C.-H.; Wang, Y. X-ray Absorption Spectroscopic Studies on Light-Induced Excited Spin State Trapping of an Fe(II) Complex.*J. Am. Chem. Soc.***2000**, *122*, 5742-5747.

[31] Mannini, M.; Pineider, F.; Sainctavit, Ph.; Joly, L.; Fraile-Rodríguez, A.; Arrio, M.-A.; Cartier dit Moulin, C.; Wernsdorfer,W.; Cornia, A.; Gatteschi, D.; *et al.*X-Ray magnetic Circular Dichroism Picks out Single-Molecule Magnets Suitable for Nanodevices. *Adv. Mater.***2009**, *21*, 167-171.

[32] Margheriti, L.; Chiappe, D.; Car, P.-E.; Sainctavit, Ph.; Arrio, M.-A.; Buatier de Mongeot, F.; Criginski Cezar, J.; Piras, F. M.; Magnani, A.; *et al.*X-Ray detected Magnetic Hysteresis of Thermally Evaporated Terbium Double-Decker Oriented Films. *Adv. Mater.***2010**, *22*, 5488-5493.

[34] Mannini, M.; Tancini, E.; Sorace, L.; Sainctavit, Ph.; Qian, Y.; Otero, E.; Chiappe, D.; Margheriti, L.; Criginski Cezar, J.; *et al.*Spin Structure of Surface-Supported Single-Molecule Magnets from Isomorphous Replacement and X-ray Magnetic Circular Dichroism. *Inorg. Chem.***2011**, *50*, 2911-2917.

[35] Brossard, S.; Volatron, F.; Lishard, L.; Arrio, M.-A.; Catala, L.; Mathonière, C.; Mallah, T.; Cartier dit Moulin, C.; Rogalev, A.; Wilhelm, F.; *et al.*Investigation of the Photoinduced Magnetization of Copper Octacyanomolybdates Nanoparticles by X-ray Magnetic Circular Dichroism.*J. Am. Chem. Soc.***2012**, *134*, 222-228.

[36] Mannini, M.; Pineider, F.; Sainctavit, Ph.; Danieli, C.; Otero, E.; Sciancalepore, C.; Talarico, A. M.; Arrio, M.-A.; Cornia, A., Gatteschi, D.; *et al.*Magnetic memory of a single-molecule quantum magnet wired to a gold surface.*Nat. Mater***2009**,*8*, 194-197.

[37] Briois, V.; Cartier dit Moulin, C.; Sainctavit, Ph.; Brouder, C.; Flank, A.-M. Full Multiple Scattering and Crystal Field Multiplet Calculations Performed on the Spin Transition $Fe^{II}(phen)_2(NCS)_2$ Complex at the Iron K and $L_{2,3}$ X-ray Absorption Edges.*J. Am. Chem. Soc.***1995**, *117*, 1019-1026.

[38] Wasinger, E. C.; de Groot, F. M. F.; Hedman, B.; Hodgson, K. O.; Solomon, E. I. L-edge X-ray Absorption Spectroscopy of Non-Heme Iron Sites: Experimental Determination of Differential Orbital Covalency.*J. Am. Chem. Soc.***2003**, *125*, 12894-12906.

[39]Hocking, R. K.; Wasinger, E. C.; de Groot, F. M. F.; Hodgson, K. O.; Hedman, B.; Solomon, E. I. Fe L-Edge XAS Studies of $K_4(Fe(CN)_6]$ and $K_3[Fe(CN)_6]$: A Direct Probe of Back-Bonding.*J. Am. Chem. Soc.***2006**, *128*, 10442-10451.

[40] Thole, B.T.; van der Laan, G. Branching ratio in x-ray absorption spectroscopy. *Phys. Rev. B***1988**, *38*, 3158-3171.

[41]van der Laan, G.; Kirkman, I. W. The 2p absorption spectra of 3d transition metal compounds in tetrahedral and octahedral symmetry.*J. Phys.: Condens. Matter***1992**, *4*, 4189-4204.

[42] Zhang, X.; Palamarciuc, T.; Rosa, P.; Létard, J.-F.; Wu, N.; Doudin, B.; Zhang, Z.; Wang, J.; Dowben, P. A. Electronic Structure of a Spin Crossover Molecular Adsorbate. *J. Phys. Chem.***2012**, *116,* 23291.

[43] One may note that the Fe(II) absorber is approximately octahedral in the LS state, but much less so in the more distorted HS state, see Guionneau, P.; Marchivie, M.; Bravic, G.; Létard, J.-F.; Chasseau, D. Structural Aspects of Spin Crossover. Example of the $[Fe^{II}L_n(NCS)_2]$ Complexes.*Top. Curr. Chem.***2004**, *234*, 97-128.

[44] See Table S2 in Supporting Information for details on that calculation.

[45] Poneti, G.; Mannini, M.; Sorace, L.; Sainctavit, Ph.; Arrio, M.-A.; Otero, E.; Criginski Cezar, J.; Dei, A. Soft-X-ray-Induced Redox Isomerism in a Cobalt Dioxolene Complex. *Angew. Chem. Int. Ed.***2010**, *49*, 1954-1957.

[46] Hauser, A. Intersystem Crossing in Fe(II) Coordination Compounds. *Coord. Chem. Rev.***1991**, *111*, 275-290.

[47] Seiler, H. Einige aktuelle Probleme der Sekundärelektronenemission. *Z. Angew. Phys.***1967**, *22*, 249-260.

[48] Ono, S.; Kanaya, K. The energy dependence of secondary emission based on the range-energy retardation power formula.*J. Phys. D.: Appl. Phys.***1979**, *12*, 619-632.

[49] Frazer, B. H.; Gilbert, B.; Sonderegger, B. R.; De Stasio, G. The probing depth of total electron yield in the sub-keV range: TEY-XAS and X-PEEM. *Surface Sci.***2003**, *537*, 161-167.

[50]T_{LIESST} temperatures are seen qualitatively to be close to 50 K, similar to the 52 K observed for the bulk in photomagnetic measurements. The LIESST measurement is a kinetic experiment, thus very sensitive to the timescale of the measurement, which is above several minutes for a XAS setup, all the more in the thermally activated regime, expected above 40 K for compound **1**.

[51]The 100 K thick film XMCD spectrum, with no contribution from compound **1**, shows a paramagnetic degradation product (Fig. S10 in Supporting Information).

[52] The absorption stems from the sum rule on the number of holes created, see Thole, B. T.; van der Laan, G.; Fabrizio, M. Magnetic ground-state properties and spectral distributions. I. X-ray-absorption spectra. *Phys. Rev. B*, **1994**, *50*, 11466-11473.

[53] Thole, B. T.; van der Laan, G. Magnetic ground-state properties and spectral distributions. II. Polarized photoemission. *Phys. Rev. B*, **1994**, *50*, 11474-11483.

[54]STM images (see Figure S12) show no evidence of aggregates, fragments of monolayersor multilayers islands. Being unable to identify isolated molecules in these measurements is not surprising: in measurements at room temperature, where the molecules may not be immobilized the way they are at cryogenic temperatures (see refs 16 and 25).Furthermore the STM setup is directly connected to the synchrotron spectrometer, which makes it difficult to perform measurements with low vibrational noise.

[55] Martin, J.-P.; Zarembovitch, J.; Dworkyn, A.; Haasnoot, J. G.; Codjovi, E. Solid-State Effects in Spin Transitions: Role of Iron(II) Dilution in the Magnetic and Calorimetric Properties of the Series $[Fe_xNi_{1-x}(4,4'\text{-bis}(1,2,4\text{-triazole}))_2(NCS)_2]\bullet H_2O$. *Inorg. Chem.***1994**, *33*, 2617-2623.

[56] Létard, J.-F.; Guionneau, P.; Nguyen, O.; Sánchez Costa, J.; Marcén, S.; Chastanet, G.; Marchivie, M.; Goux-Capes, L. A Guideline to the Design of Molecular-Based Materials with Long-Lived Photomagnetic Lifetimes.*Chem. Eur. J.***2005**, *11*, 4582-4589.

[57]Sanvito, S. Molecular spintronics. *Chem. Soc. Rev.***2011**, *40*, 3336-3355.

Supporting Information

Temperature- and Light-Induced Spin Crossover Observed by X-Ray Spectroscopy on Isolated Fe(II) Complexes on Gold

Ben Warner,[⊥†] Jenny C. Oberg,[⊥†] Tobias G. Gill,[⊥ǂ] Fadi El Hallak,[⊥] Cyrus F. Hirjibehedin,[⊥†‡] Michele Serri, [#] Sandrine Heutz,[#] Marie-Anne Arrio,[&] Philippe Sainctavit,[&] MatteoMannini,[§] Giordano Poneti,[§¦] Roberta Sessoli[§] and Patrick Rosa[*‖]

⊥ London Centre for Nanotechnology, University College London, London (UK)

† Department of Physics & Astronomy, University College London, London (UK)

ǂ Department of Chemistry,University College London, London (UK)

#Department of Materials and London Centre for Nanotechnology, Imperial College London, London (UK)

&Institut de Minéralogie et de Physique des Milieux Condensés, UMR7590, Université Pierre et Marie Curie, Paris (France)

§La.M.M, Department of Chemistry & INSTM Research Unit, Università di Firenze, Florence (Italy)

¦Department of Applied Sciences and Technology, Guglielmo Marconi University, Rome (Italy)

‖ CNRS, Univ. Bordeaux, ICMCB, UPR 9048, F-33600 Pessac, France

Contents

Experimental details

Single crystals of complex [Fe($H_2B(pz)_2)_2$(bipy)] **1** were obtained as described previously.[1] For the bulk measurement, one single crystal of compound **1** was crushed between two pieces of 99.999% pure Au foil (Goodfellow), and the excess shaken off. A 300 nm thick film of compound **1** was thermally evaporated on polycrystalline Cu foil under high vacuum (1,9.10^{-6} mbar) from a ceramic crucible filled with 150 mg of single crystals and heated up to 130°C in a Kurt J. Lesker SPECTROS organic molecular beam deposition (OMBD) system (Imperial College). A K-type thermocouple connected to the crucible measured its temperature during the whole process. The apparatus was equipped with a cold cathode and a quartz crystal microbalance, thus allowing the real-time monitoring of both the pressure variations and the thickness of the deposited film. *In situ* experiments at the ESRF (Grenoble, France) used a similar crucible, under ultra-high vacuum at the same temperature of 130°C.[2]Sub-monolayer coverage was achieved with a 30 min evaporation (no quartz microbalance was available to monitor the deposition rate, that varies not only with the temperature-dependent evaporation rate but also with the solid angle between crucible and substrate).Au(111) single crystal samples were prepared in UHV by repeated cycles of sputtering with Ar and annealing to 500°C for 20 min.

XAS/XMCD measurement details

XAS and XMCD measurements were performed at the ID08 beamline at the ESRF synchrotron facility (Grenoble, France).[3] Samples were inserted in a sample holder screwed to the coldfinger of a ^{4}He cryostat working down to 7 K. Spectra were recorded at Fe-$L_{2,3}$ edges (2p-3d transitions). Laser illumination was performed by illuminating the sample from an external window using a *cw* 658 nm laser diode aligned on the sample surface after sample cooling down.All measurements were carried out at very low X-rays photon flux (flux reduced around 500 times compared to the maximum photon flux of ID08 beamline), so as to avoid radiation damage,[4] and we used the

---

[1] Palamarciuc, T.; Oberg, J. C.; El Hallak, F.; Hirjibehedin, C. F.; Serri, M.; Heutz, S.; Létard, J.-F.; Rosa, P. *J. Mater. Chem.***2012**, *22*, 9690-9695.

[2] It must be noted that molecules of compound **1** do not stand prolonged heating. Analysis of the residue left in the crucible (see ref 1 for the methods used) showed the loss of the SCO properties and a change in chemical composition. We suspect other SCO compounds may be similarly heat-sensitive.

[3] Goulon, J.; Brookes, N. B.; Gauthier, C.; Goedkoop, J. B.; Goulon-Ginet, C.; Rogalev, M. *Phys. B. Condens. Matter***1995**, *208/209*, 199-202.

[4]a) M. Mannini *et al.*, *Adv. Mater.***2009**, *21*, 167-171; b) L. Margheriti *et al.*, *Adv. Mater.***2010**, *22*, 5488-5493; c) M. Mannini *et al.*, *Nature***2010**, *468*, 417-421; d) M. Mannini *et al.*, *Inorg. Chem.***2011**, *50*, 2911-2917; e) S. Brossard *et al.*, *J. Am. Chem. Soc.***2012**, *134*, 222-228: f) M. Mannini *et al.Nat. Mater* 2009,8, 194-197.

Total Electron Yield (TEY) detection mode in order to achieve the required surface sensitivity, giving an estimated sampling depth on the order of 5 nm.[5] XMCD spectra were evaluated as (σ^--σ^+), where σ^- and σ^+ are the measured cross sections for right and left circularly polarized light when the external magnetic field is parallel to the X-ray propagation vector. Given this sign convention, the signal is negative at the L_3 edge when the iron magnetic moment is parallel to the external magnetic field.To minimize systematic errors, each XMCD spectrum was obtained from eight measurements taken by switching the polarization and the field.[6] (σ^- + σ^+)/2 was considered a good approximation to the isotropic spectrum in the electric dipole approximation since no sizeable X-ray linear dichroism was observed. All reported XMCD contributions are normalized by dividing the measured XMCD signal by the edge-jump of the isotropic absorption spectra at the energy of its maximum amplitude.

XAS/XMCD ligand field multiplet calculations

In the electric dipole approximation, $L_{2,3}$ edges probe transitions from the 2p core levels to 3d states (and with a weaker probability to 4s). For 3d metals, they are sensitive mainly to the atomic electronic structure of the absorber and can be thus calculated by using the Ligand Field Multiplet code developed by Thole[7] in the framework established by Cowan[8] and Butler.[9]This approach takes into account the multielectronic Coulomb repulsions, the 3d and 2p spin-orbit coupling, spin and orbit contributions to the Zeeman Hamiltonian, and treats the geometric environment of the absorbing atom by an electrostatic potential.[10] The spectrum is calculated as the sum of all possible transitions for an electron jumping from the 2p to the 3d level in the electric dipole approximation. The electric dipole allowed 2p to 4s transitions are calculated and found negligible. Multielectronic repulsions are introduced through the Slater Integrals calculated within an atomic Hartree-Fock model.For the Fe(II) $L_{2,3}$ edge in compound **1**, the Slater integrals were scaled down by a κ = 80% reduction factor to account for the electronic delocalization. The coordination sphere of the Fe(II) ions was described by an octahedral crystal field with respectively 10Dq = 1eV for the HS state, and 2.2eV for the LS state. The spin-orbit coefficients are Hartree-Fock calculated ones.

---

[5] R. Nakajima, J. Stohr, Y. U. Idzerda, *Phys. Rev. B***1999**, *59*, 6421-6429.
[6] R. Sessoli, M. Mannini, F. Pineider, A. Cornia, Ph. Sainctavit, in *Magnetism and Synchrotron Radiation*, *Springer Proceedings in Physics*, Vol. 133 (Eds: E. Beaurepaire, H. Bulou, F. Scheurer, J. P. Kappler), SPRINGER-VERLAG, Berlin, **2010**, p 279.
[7] B.-T. Thole, G. van der Laan, J. C. Fuggle, G. A. Sawatzky, R. C. Karnatak, J.-M. Esteva, *Phys. Rev. B***1985**, *32*, 5107-5118.
[8] R. D. Cowan, *The Theory of Atomic Structure and Spectra*, University of California Press, Berkeley **1981**.
[9] P. H. Butler, *Point Group Symmetry, Applications, Methods and Tables*, Plenum, New York **1991**.
[10] F. M. F. de Groot, J. C. Fuggle, B. T. Thole, G. A. Sawatzky, *Phys. Rev. B***1990**, *42*, 5459-5468.

The calculated line spectra were convolved with Voigt profiles: [11] σ = 0.1 eV for instrumental broadening, Γ_3 = 0.2 eV at the L_3 edge and Γ_2 = 0.4 eV at the L_2 edge.

We decided to perform the LFM calculations within a single configuration model. Doing so, one limits the number of empirical parameters at the expense of not reproducing exactly all the observed experimental features. Other authors (Lee al. JACS 2000) [12] have shown that the incorporation of extra configurations within the MLCT model was accompanied by a better simulation of shoulders present on $L_{2,3}$ edges. Nevertheless the increase of parameters does not yield more information on the electronic structure of the iron ions as can be noticed from their paper.

Magnetic measurements

Magnetic measurements were performed on a MPMS-7 Quantum Design SQUID magnetometer (10-250 K, 10 kOe), on powder samples sealed in 30 μm-thick polyethylene bags and accurately weighed with a Mettler MX5 microbalance. Photomagnetic measurements were performed with a Laser diode Oxxius OXV-375 (λ = 375 nm, 15 mW) coupled by an optical fibre to the sample cavity, the power available the sample surface being measured at 5 mW.cm^{-2}. Results were similar using a Spectrum Physics Series 2025 Ar^+/Kr^+ laser (λ = 514,647 nm, adjustable output).

[11] Briois, V.; Cartier dit Moulin, C.; Sainctavit, Ph.; Brouder, C.; Flank, A.-M. *J. Am. Chem. Soc.***1995**, *117*, 1019-1026.
[12] Lee, J.-J.;*et al.J. Am. Chem. Soc.***2000**, *122*, 5742-5747.

Figure S1:Bulk and thick film variation of the $L_{2,3}$ edge X-ray absorption spectra with temperature.

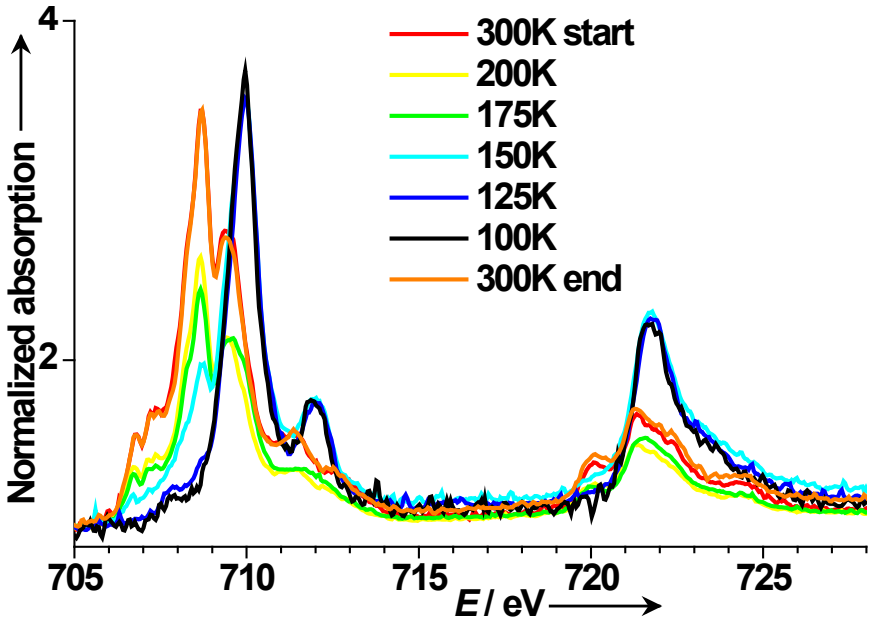

Temperature evolution of the normalized spectra (pre-edge) for the bulk (scratched single crystal on Au foil).

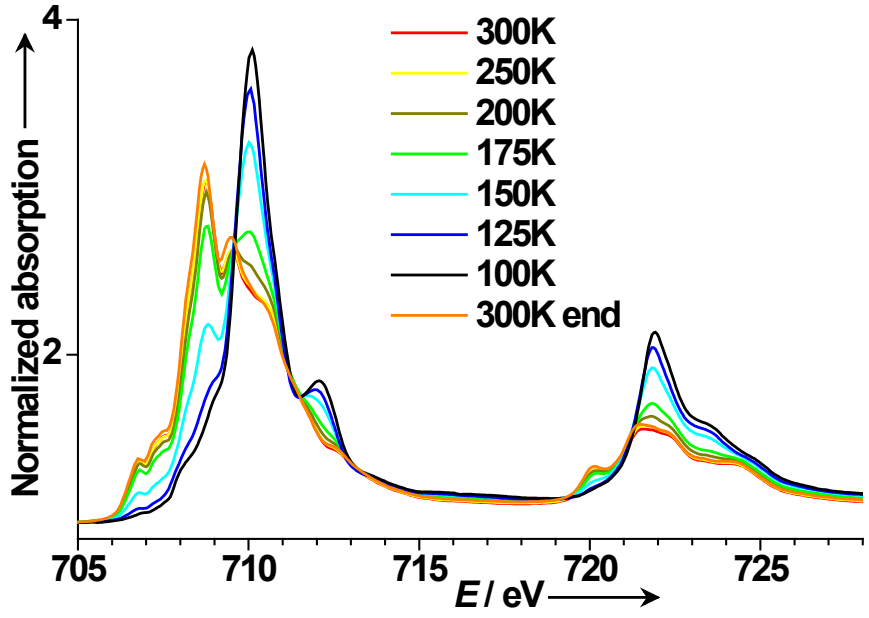

Temperature evolution of the normalized spectra (pre-edge) for the 300 nm thick film on Cu foil

Table S2:Deconvolution results for the bulk spectra

Spectra were deconvoluted as a.spectrum(300 K) +b.spectrum(100 K) +c. The offset c is not reported here

T (K)	n_{HS} (%)	n_{LS} (%)	a	b	r^2	Comments
300	100.0	0.0	1	0		
100	0.0	100.0	0	1		
10	1.5(8)	98.5(13)	0.02(1)	1.29(1)	0.967	
10	97.4(14)	2.6(8)	1.75(1)	0.05(1)	0.965	laser 658 nm ON for 90 min
10	92.9(12)	7.1(7)	1.41(1)	0.11(1)	0.972	Measurement at +50 kOe only
15	95.3(12)	4.7(7)	1.73(1)	0.08(1)	0.972	Measurement at +50 kOe only
30	95.9(18)	4.1(11)	1.91(2)	0.08(2)	0.942	Measurement at +50 kOe only
35	92.0(16)	8(1)	1.91(2)	0.17(2)	0.951	Measurement at +50 kOe only
40	85.9(16)	14.1(10)	1.62(2)	0.26(2)	0.942	Measurement at +50 kOe only
45	72.2(13)	27.8(10)	1.29(2)	0.50(2)	0.945	Measurement at +50 kOe only
50	31.3(8)	68.7(7)	0.57(1)	1.25(1)	0.963	Measurement at +50 kOe only
100	--	100.0(4)	--	1.631(6)	0.988	
125	1.0(5)	99.0(8)	0.014(7)	1.173(8)	0.987	
150	21.1(5)	78.9(8)	0.313(7)	1.173(7)	0.984	
175	79.5(4)	20.5(3)	1.343(5)	0.345(5)	0.995	
200	96.0(6)	4.0(4)	1.700(7)	0.071(7)	0.992	
300	100.5(8)	-0.5(5)	1.624(7)	-0.009(7)	0.990	

$r^2 = 1 - {\sum_{i=1}^{n}(y_i - y_i^{calc})^2}/{\sum_{i=1}^{n} y_i^2}\ {n-1}/{n-3}$ where n is the number of experimental points

Mössbauer studies on the bulk compound (as powder) showed some 10% residual LS above 250 K, while a complete LS state was reached at 80 K.[13] The differences seen in the spectra of the bulk we measured (as a scratched single crystal) at 300 and 100 K, and the perfect agreement with calculated spectra, preclude such a large LS residue at 300 K. Such differences are nevertheless quite usual between microcrystals and macroscopic single crystals for SCO compounds.

We found in our magnetic measurements of the bulk a $\chi_M T$ value at 250 K of 3.72 $cm^3.K.mol^{-1}$, higher than the one reported in ref 13 (3.6 $cm^3.K.mol^{-1}$). We used this value as representative of the 100% HS state, not considering the Mössbauer data, to obtain the n_{HS} fractions as $n_{HS}(T) = {\chi_M T}/{3.72}$

Please note that the SOXIESST effect observed at 10 K that is smaller than for the other two samples reported here is due to the fact that the bulk reference was exposed to the X-Ray beam for a shorter time than the thick and thin film samples at that temperature prior to visible light irradiation.

[13]N. Moliner *et al.*, *J. Phys. Chem. B*, **2002**, *106*, 4276-4283.

Below are illustration of the fit result at 150 K and 50 K: experimental spectrum (black line), fit (red line), HS (blue line) and LS (green line) components.

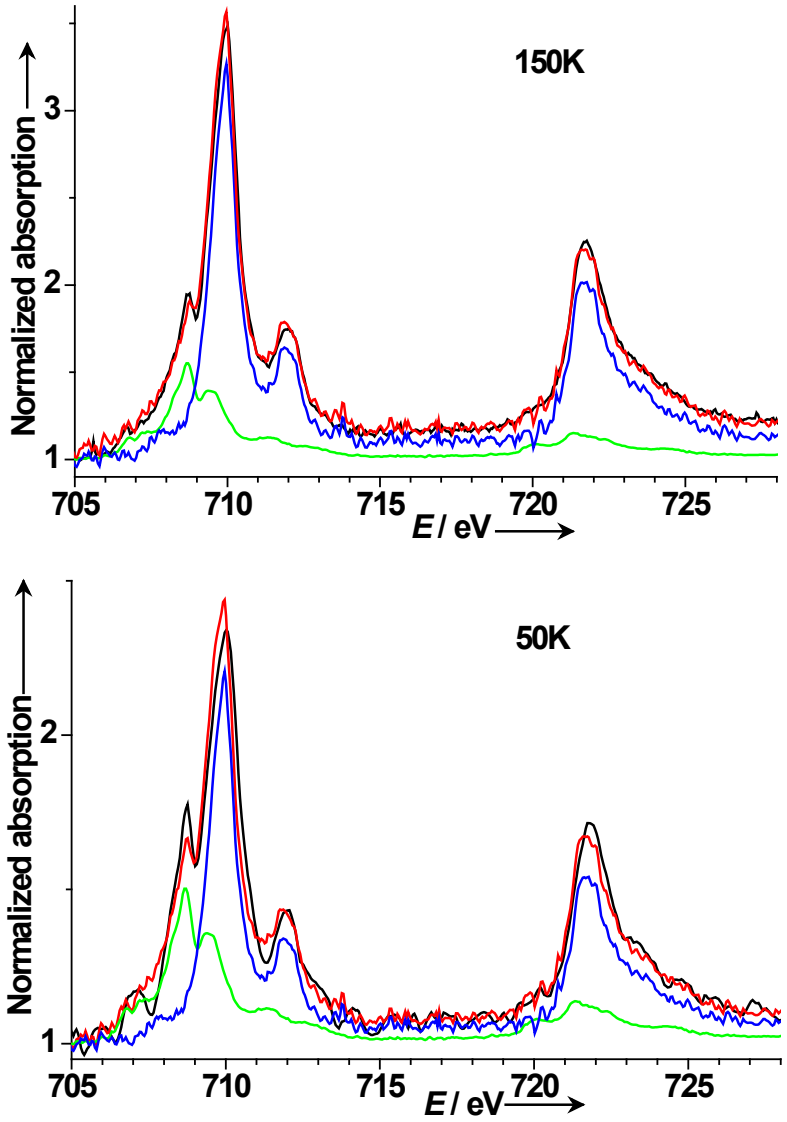

Figure S3:Deconvolution of 300 K and 100 K spectra for the thick film

The 300 K (black line) and 100 K (blue line) were adjusted manually with respectively the 300 K and 100 K bulk spectra together with a linear baseline (upper red and green lines), until similar residues (lower red and green lines) were obtained. The average of those residues was then considered as a spurious contribution due to some impurity present in the bulk deposit, and used as such for the deconvolution of the thick film spectra. The reconstituted spectrum is quite dependent on the reference LS spectrum, since its main feature is very close to the main L_3 absorption peak of the LS spectrum, with some resulting artefacts. Analysis errors for the thick film were accordingly increased (see Table S5).

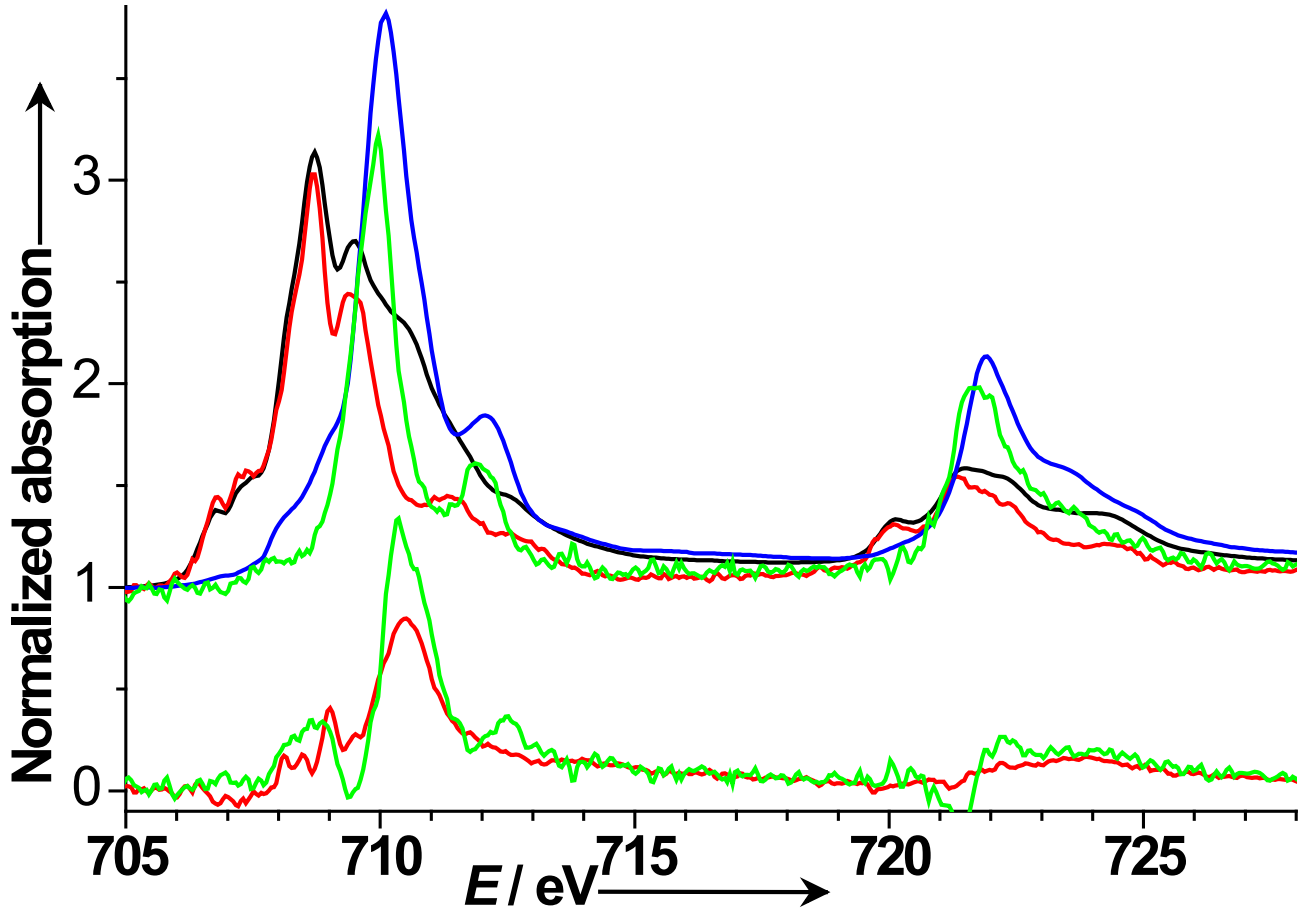

Figure S4:Comparison of the bulk and spurious contribution spectra

300 K (black line) and 100 K (red line) normalized (pre-edge) spectra for the bulk compound are represented together with the extracted spectrum for the spurious contribution(blue line). The latter pre-edge was normalized likewise.

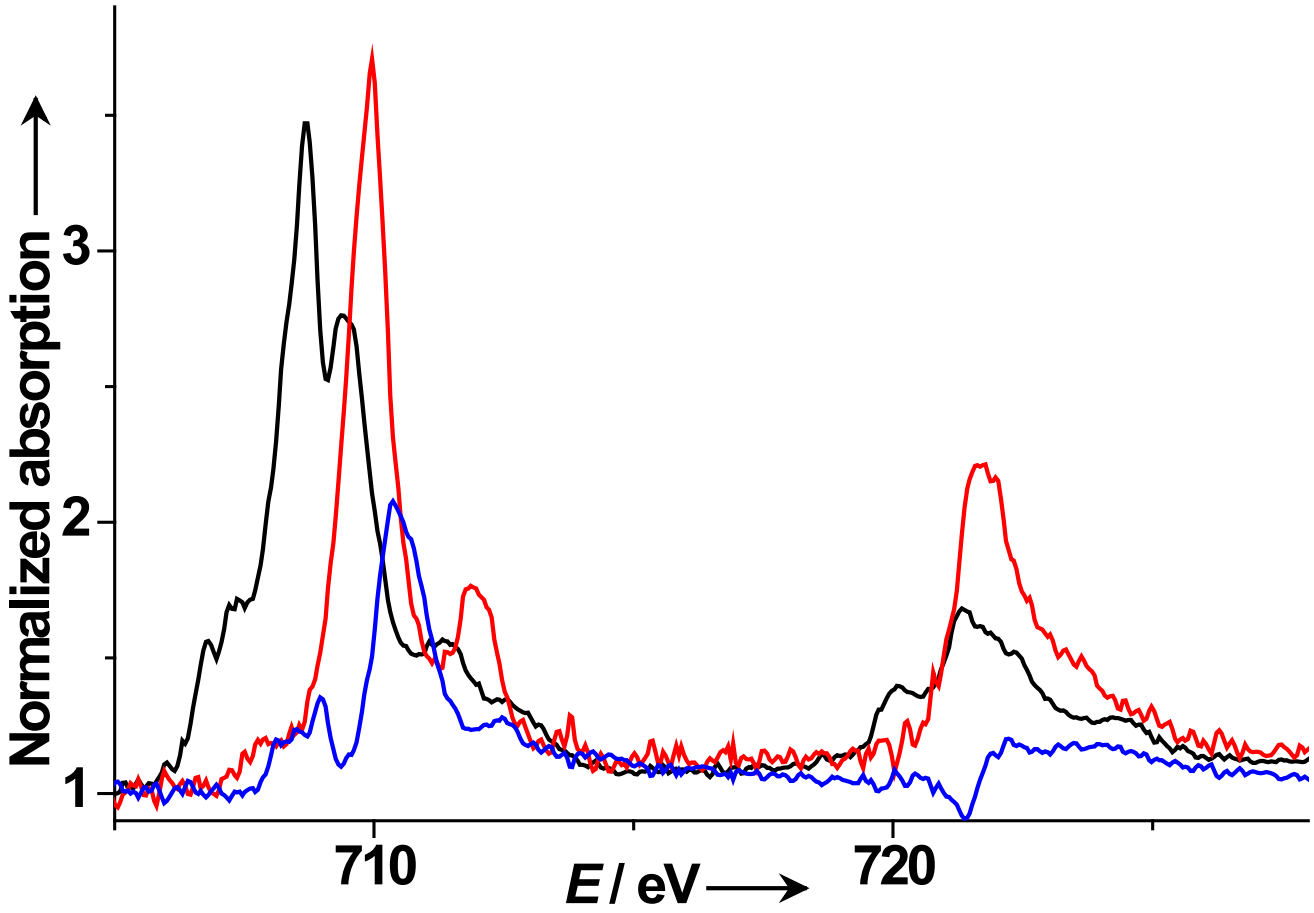

Table S5:Deconvolution results for the thick film

After substraction of the spurious contribution, thick film spectra were deconvoluted as a.spectrum(bulk 300 K) + b.spectrum(bulk 100 K) + c. The offset c is not reported here. It was previously checked that a full deconvolution considering a variable spurious contribution yielded a resulting coefficient quite close to 1 (between 0.76 and 1.23). Nevertheless errors resulting from the multilinear regression fit are clearly underestimated, since the unknown component spectrum is itself quite dependent itself on the reference LS spectrum. Upon some trials we multiplied accordingly those errors by a factor of 4.

T (K)	n_{HS} (%)	n_{LS} (%)	a	b	r^2	Comments
300	99.5(36)	0.5(21)	0.820(4)	0.004(4)	0.985	
100	0.9(21)	99.1(36)	0.007(4)	0.827(4)	0.997	
10	11.3(21)	88.7(33)	0.094(4)	0.736(4)	0.985	
300	96.9(37)	3.1(22)	0.766(4)	0.024(4)	0.984	
250	96.0(35)	4.0(21)	0.765(4)	0.032(4)	0.985	
200	86.9(30)	13.1(19)	0.701(3)	0.105(4)	0.987	
175	73.2(20)	26.8(15)	0.598(3)	0.219(3)	0.992	
150	36.8(6)	63.2(7)	0.306(1)	0.526(1)	0.999	
125	12.5(9)	87.5(14)	0.102(2)	0.720(2)	0.997	
50	10.0(12)	90.0(19)	0.079(2)	0.710(2)	0.995	
10	24.2(10)	75.8(14)	0.190(2)	0.592(2)	0.996	
10	100.6(59)	-0.6(34)	0.860(7)	-0.005(7)	0.964	laser 658 nm ON for 15 min
10	87.2(44)	12.8(28)	0.686(5)	0.100(5)	0.973	Measurement at +50 kOe only
20	85.9(41)	14.1(27)	0.679(5)	0.112(5)	0.976	Measurement at +50 kOe only
30	84.6(37)	15.4(24)	0.669(5)	0.122(5)	0.979	Measurement at +50 kOe only
35	80.9(33)	19.1(23)	0.642(4)	0.151(4)	0.982	Measurement at +50 kOe only
40	75.8(28)	24.2(20)	0.602(4)	0.192(4)	0.986	Measurement at +50 kOe only
42.5	68.9(23)	31.1(18)	0.549(3)	0.248(3)	0.989	Measurement at +50 kOe only
45	58.9(18)	41.1(16)	0.471(3)	0.329(3)	0.992	Measurement at +50 kOe only
47.5	45.2(12)	54.8(13)	0.363(2)	0.439(2)	0.995	Measurement at +50 kOe only
50	32.0(10)	68.0(13)	0.257(2)	0.546(2)	0.996	Measurement at +50 kOe only
55	19.4(10)	80.6(15)	0.156(2)	0.646(2)	0.996	Measurement at +50 kOe only
60	13.9(11)	86.1(17)	0.112(2)	0.695(2)	0.996	Measurement at +50 kOe only

Magnetic measurements on thick films of compounds **1** on Kapton[1] showed a linear dependence with temperature below the SCO, not seen in the bulk. This can be accounted for by ferromagnetic impurities, improving notably the agreement with the bulk behaviour, and support our observation here of some degradation of the complex upon evaporation.

Below are illustration of the fit result at 150 K and 50 K: experimental spectrum (black line), fit (red line), HS (blue line), LS (green line) and spurious (magenta line) components.

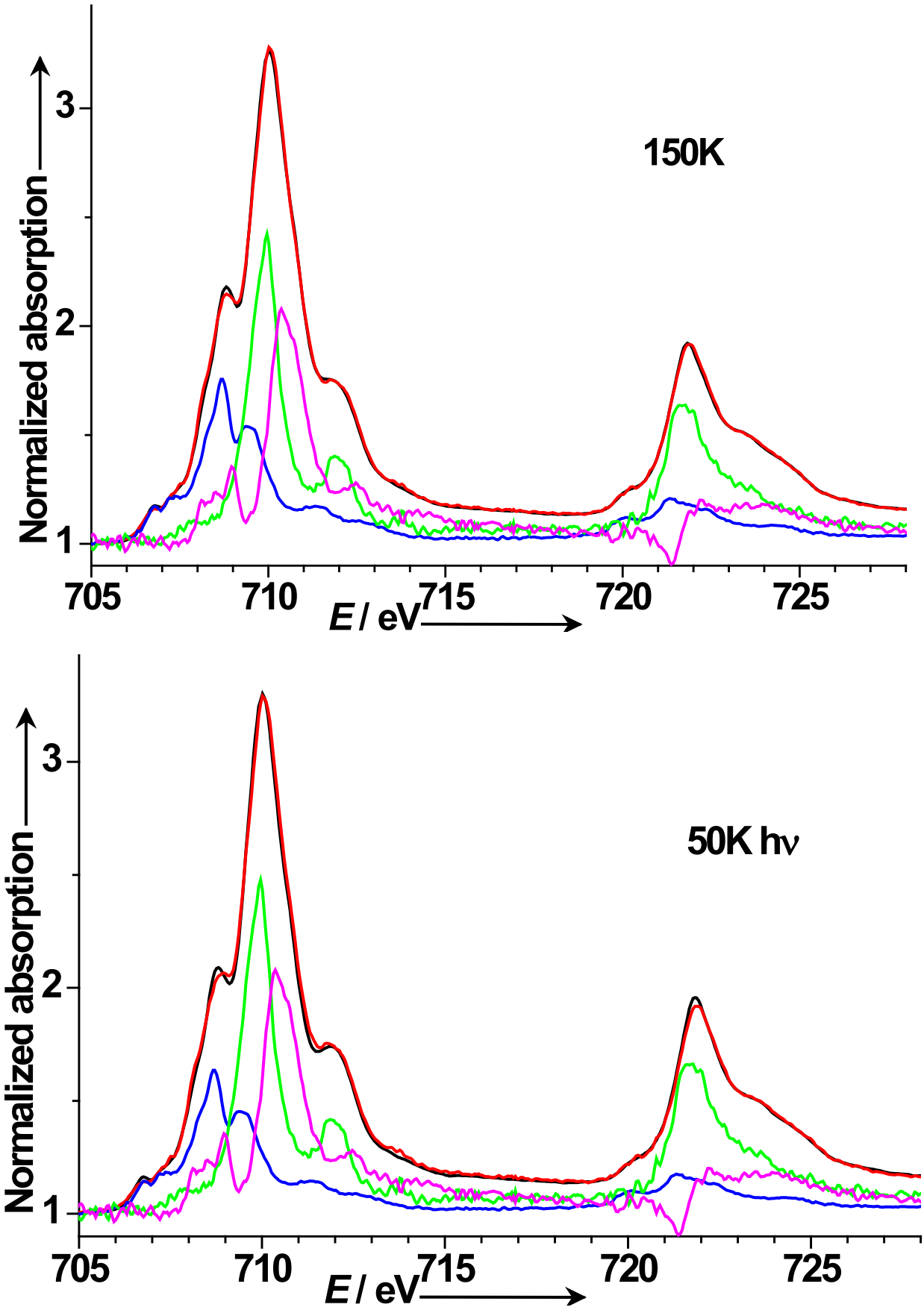
150K
Normalized absorption
1
2
3
705
710
715
720
725
E / eV
50K hν
Normalized absorption
1
2
3
705
710
715
720
725
E / eV

Figure S6:Relaxation with increasing temperature of the photoinduced HS state as monitored by the $L_{2,3}$ edge X-ray absorption spectra variation.

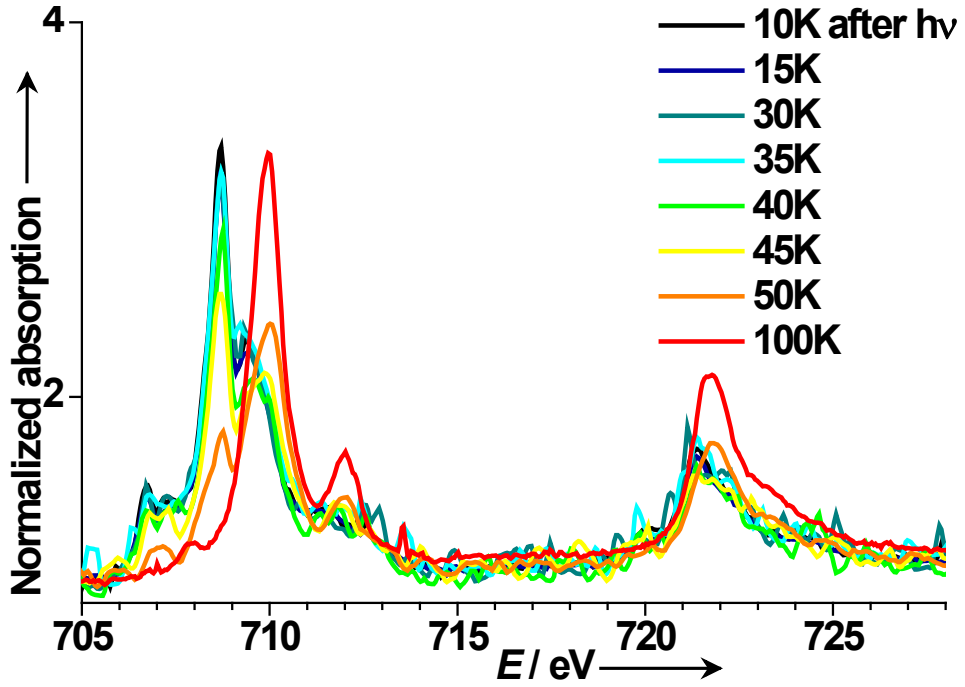

Relaxation of the photoinduced HS state monitored by the evolution of the normalized spectra (pre-edge) with temperature for the bulk (scratched single crystal on Au foil).

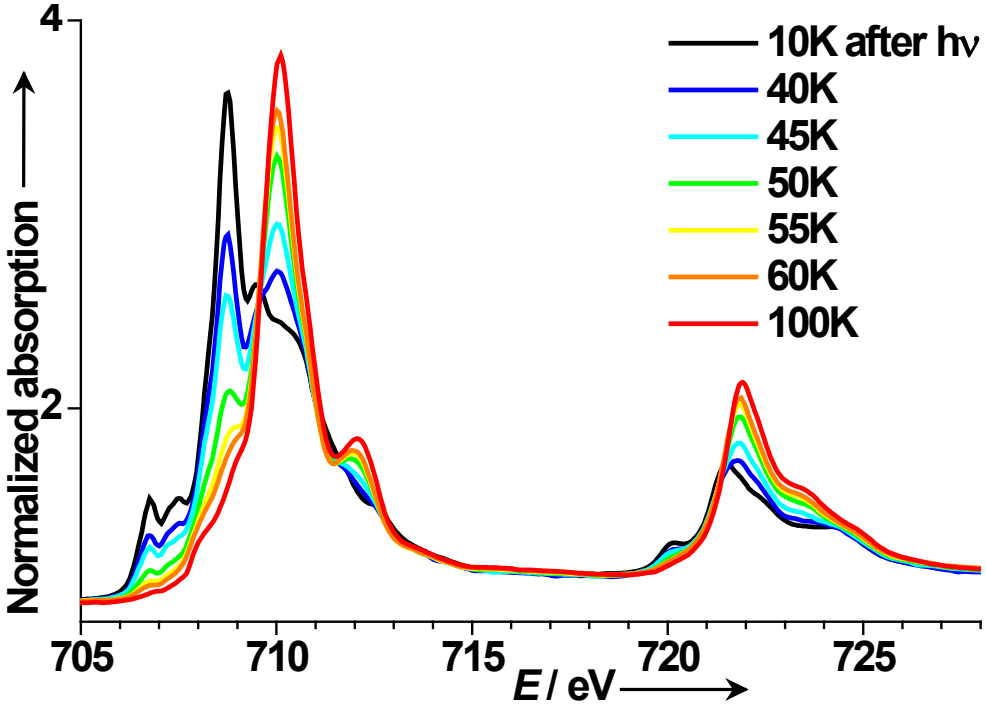

Relaxation of the photoinduced HS state monitored by the evolution of the normalized spectra (pre-edge) with temperature for the 300 nm thick film on Cu foil.

Figure S7:XMCD spectra for the thick film.

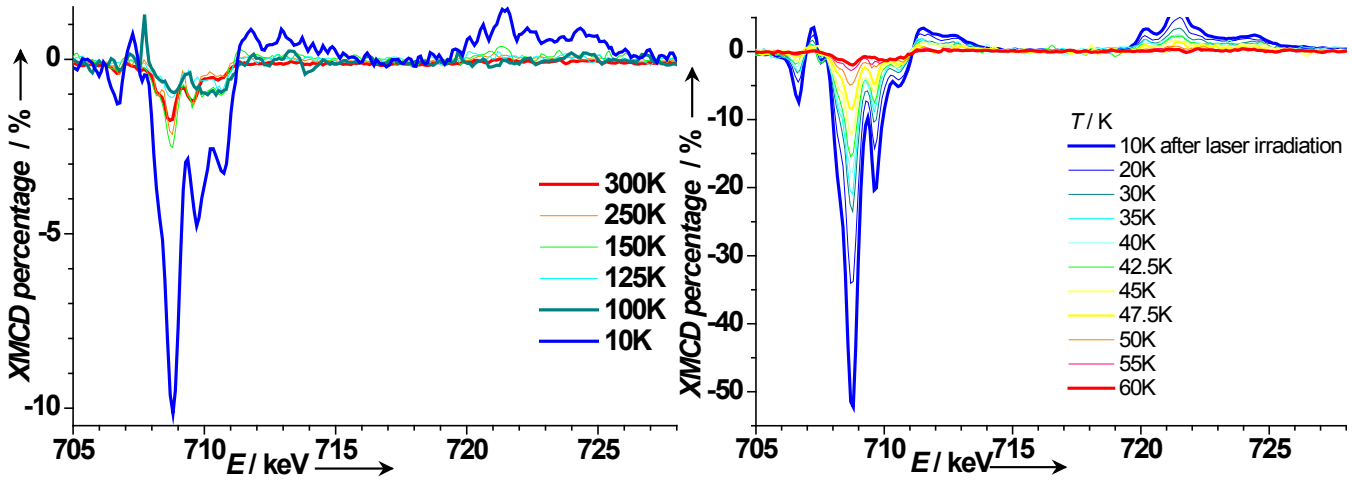

Left: Temperature evolution of the thick film XMCD spectra,from 300 to 10 K showing SCO and SOXIESST. Right: Temperature induced relaxation of the light induced HS state in the thick film as monitored from the XMCD spectra. Spectra were normalized relatively to the edge-jump of the isotropic absorption spectra at the energy of its maximum amplitude.

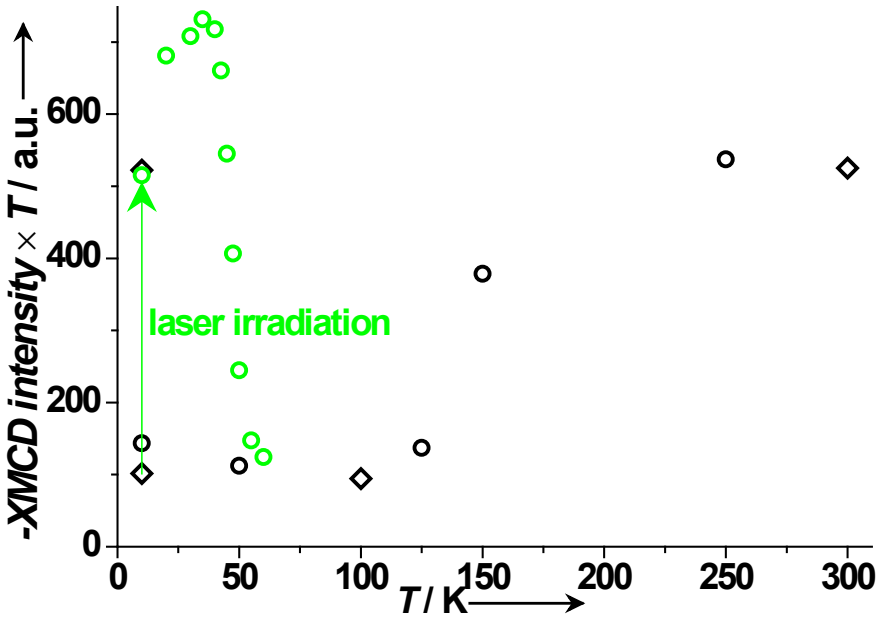

The XMCD signal is proportional to the sample local magnetic moment. For a paramagnet this moment is parallel to the magnetic field, giving thus a negative signal, and follows a Curie law. The product of the XMCD maximum signal with temperature reproduces thus the thermal SCO, the light induced photoexcitation and the relaxation towards the LS state.

Figure S8:Light induced SCO at 10 K for the bulk evidenced by the XMCD spectra.

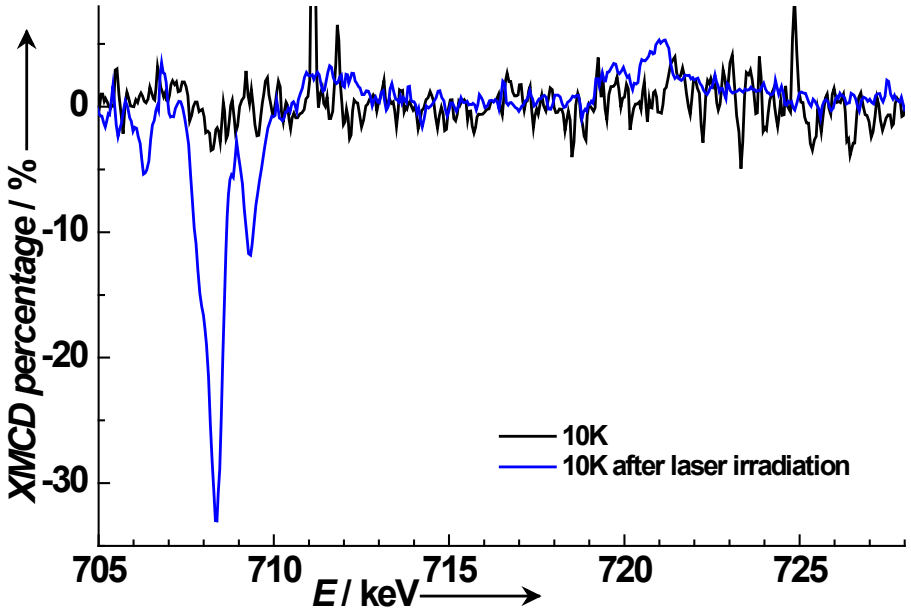

Bulk XMCD spectra, normalized relatively to the edge-jump of the isotropic absorption spectra at the energy of its maximum amplitude, at 10 K before and after laser irradiation.

Figure S9:XAS and XMCD spectra for the bulk and the thick film as compared to multiplet calculations.

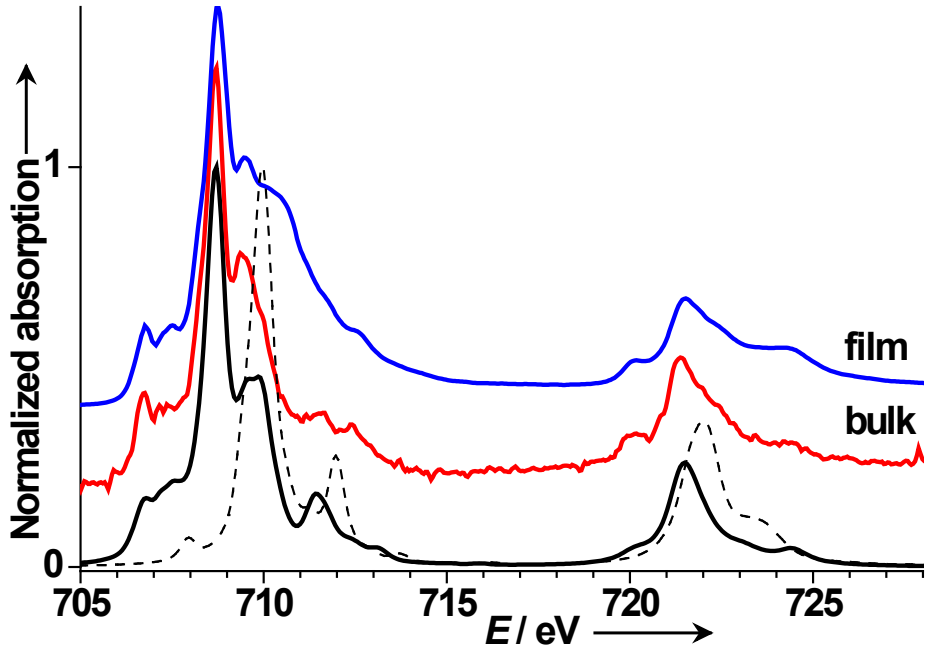

Normalized spectra (absorption maximum) for the 300 nm thick film (blue line) and the bulk (red line) at 10 K: after illumination, with calculated spectra for the HS (full black line) and LS (dashed black line) states. Spectra were vertically shifted for clarity.

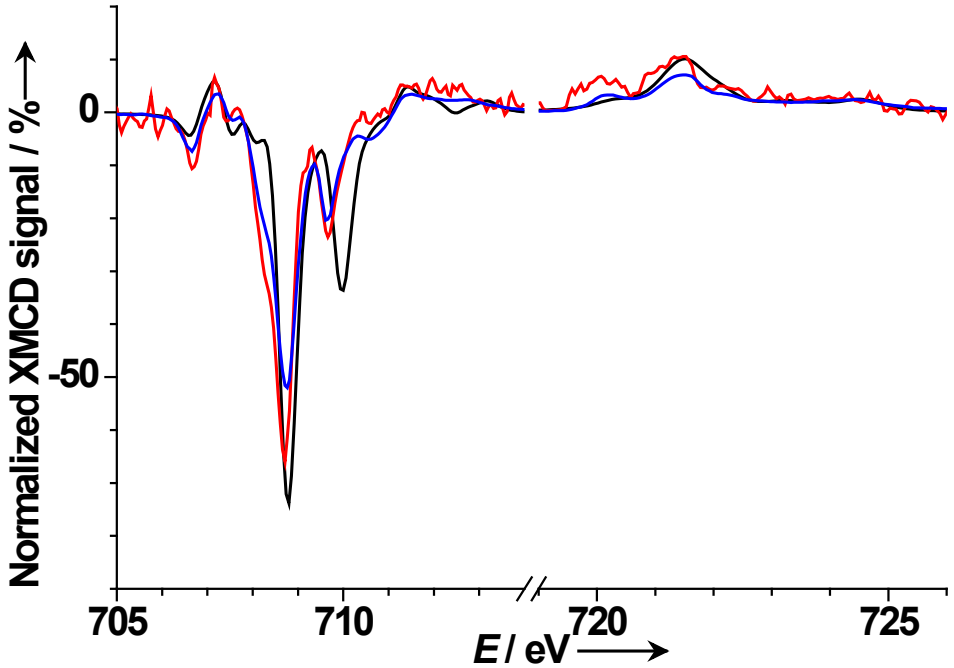

XMCD spectra, normalized relatively to the edge-jump of the isotropic absorption spectra at the energy of its maximum amplitude, at 10 K after laser irradiation, for the bulk (red line) and the thick film (blue line), together with the calculated spectrum (black line).

Figure S10:Reconstituted XAS and XMCD spectra for the degradation product.

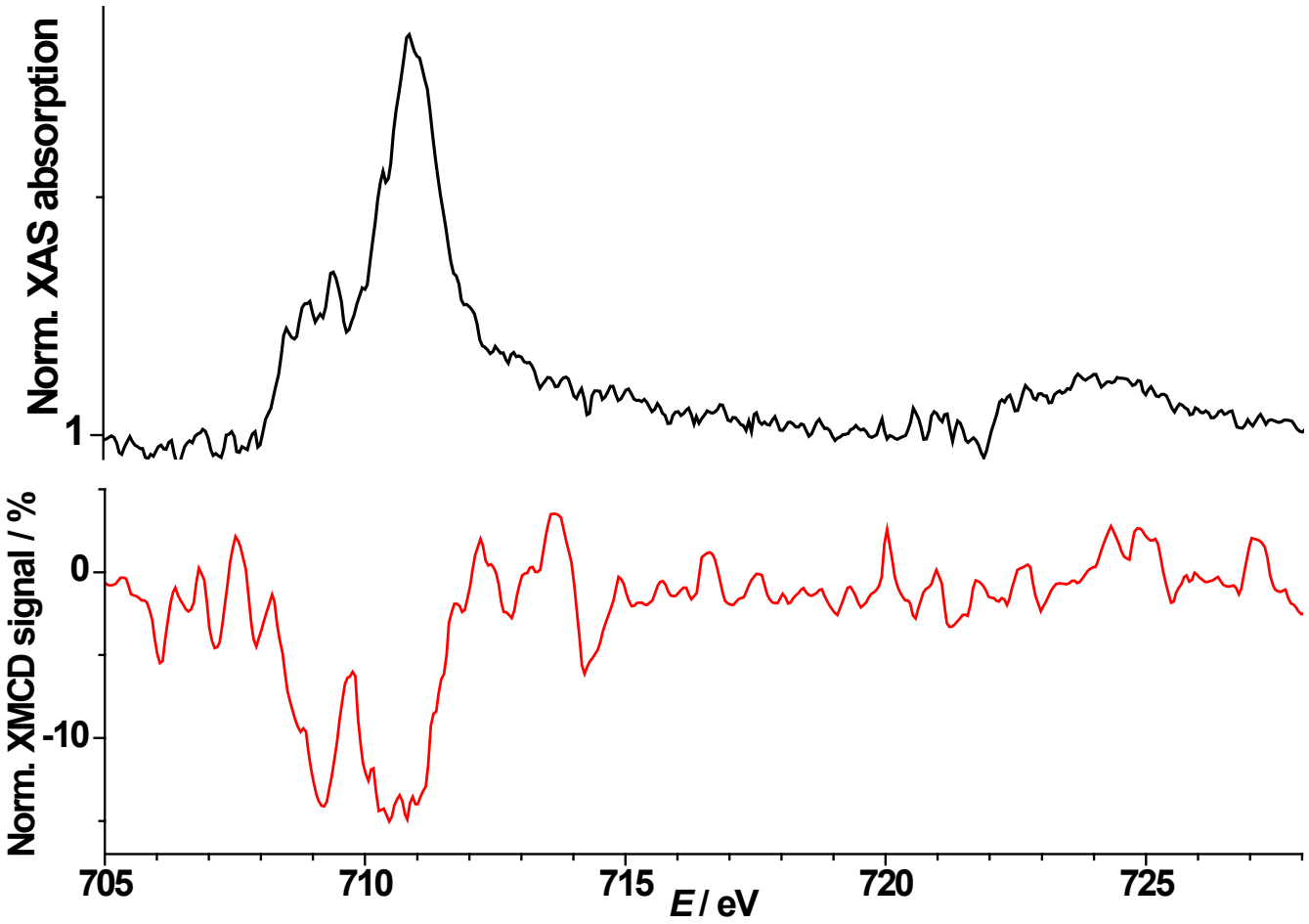

(top) Normalized (pre-edge) XAS spectrum of the degradation product reconstitued from the 100 K thick film and bulk spectra; (bottom) corresponding XMCD spectrum, normalized relatively to the edge-jump of the isotropic absorption spectra at the energy of its maximum amplitude.

Figure S11: Comparison of edge jumps on non-normalized XAS spectra

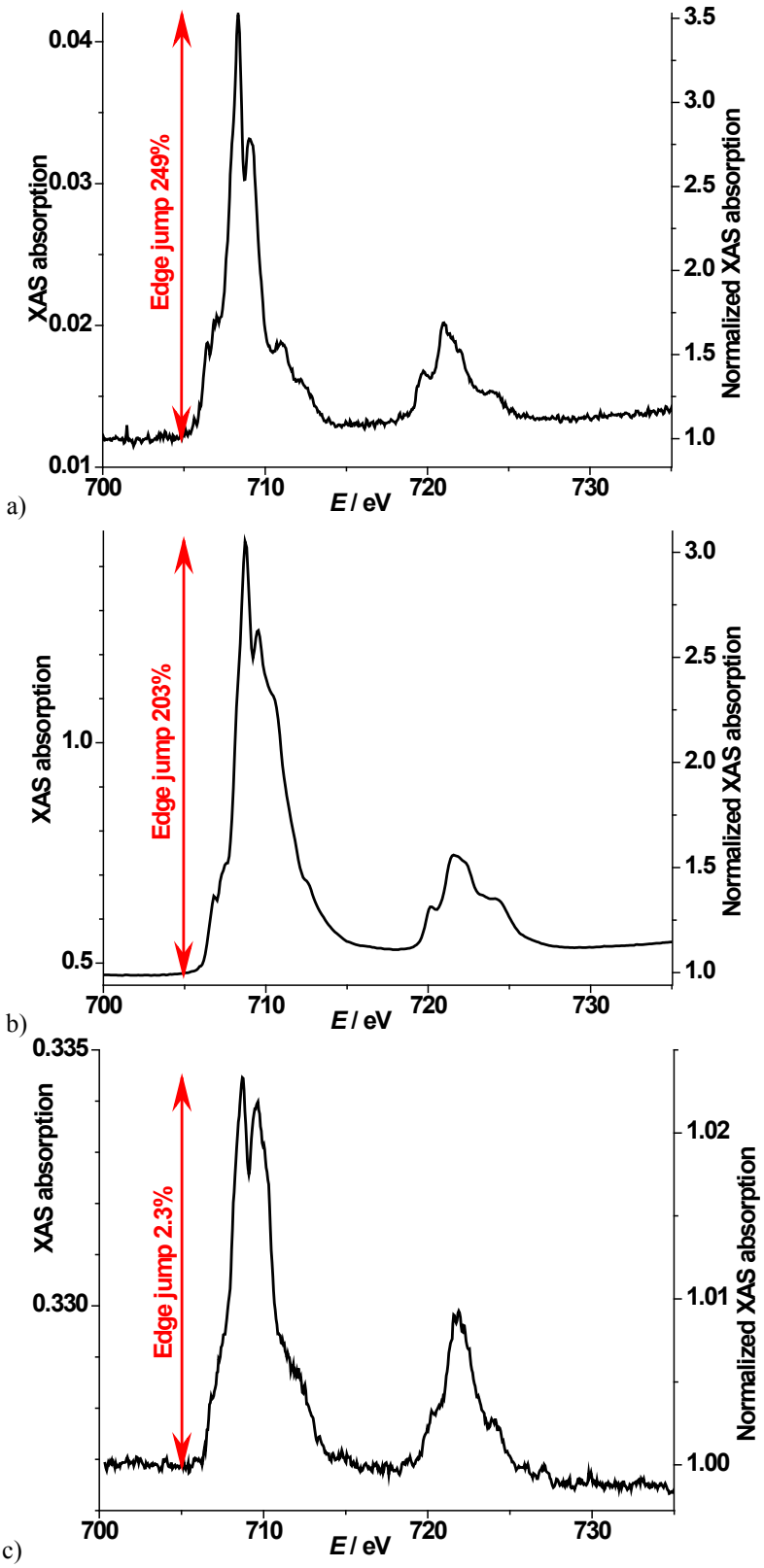

Raw XAS signal (ratio I/I_0 of electrometer counts *vs.* E) at 300 K for the bulk (a), the thick film (b) and the sub-monolayer coverage (c). For clarity, on each figure right-hand side is reported the scale after normalization relative to pre-edge (705 eV).

Note that the low pre-edge signal seen for the bulk is due to the thickness of the compound and its shielding effect. Thick film and sub-monolayer coverages were otherwise measured in two different runs, which explains the lower pre-edge signal seen for the less shielded sub-monolayer coverage. Edge jumps, calculated as the ratio of signal before and after the L_3 edge, for the bulk and the thick film are 249 and 203% respectively, to compare with the 2.3% measured for the sub-monolayer coverage. As we discussed in our previous report,[1] the film growth on copper may be epitaxial with a [11-1] preferential orientation (work is in progress to fully elucidate this point). Along this direction, according to the reported crystal structure at room temperature, we find a thickness of 8.679Å per layer of complex. This thickness is comparable to the 7.393Å per layer for the likely orientation along [200] found for the film on glass.

The XAS probing depth is typically 5 nm, value that has been found by most people trying to measure the escape depth experimentally (depending on papers it is in between 3 nm and 10 nm). This is just a rough estimate. Whether the electron escape depth is larger for metals or non metals is not clear since the average kinetic energy of the electrons is 3 to 5 eV, well above the Fermi energy. For large gap insulators (8 eV for Al_2O_3 corundum), the escape depth is believed to remain around 5 nm. This would be attributed to the presence of surface defects that completely change the band structure.

Considering that range of escape depths, we have then for the thick film an edge jump corresponding to between 3.5 and 13.5 layers of complex (the edge jump for the bulk is logically bigger, since we have crystallites without preferential orientation). So for the last sample, with an edge jump 100 times smaller we can confidently conclude that the coverage should not exceed 0.03to 0.14 monolayers.

Figure S12:STM images of the submonolayer sample

STM imaging at 300 K of compound **1** evaporated on Au(111) (30 min, 130°C).

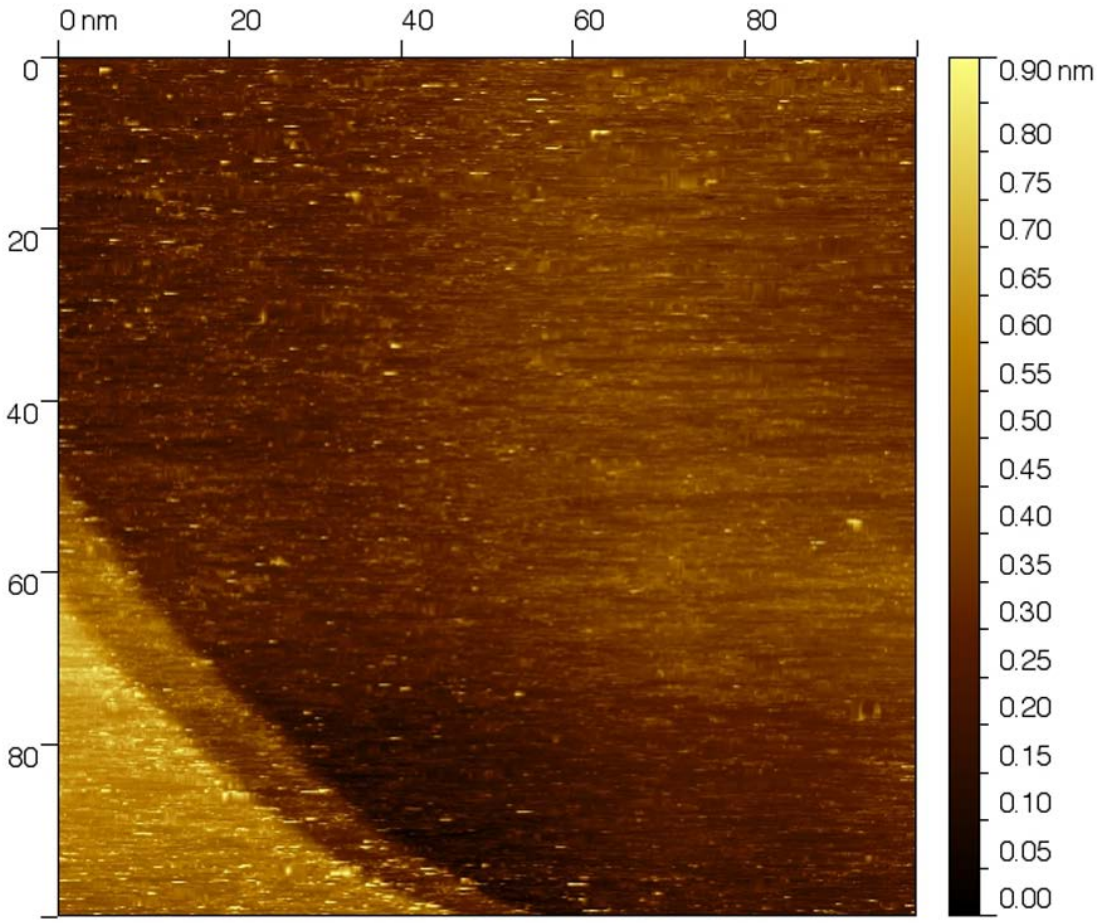

We used Scanning Tunneling Microscopy to image*in situ* without breaking the UHV the sample we had just measured. Although the XAS spectra proved that a homogeneous coverage of the surface is seen, and that indeed molecules of compound **1** are present and active on the surface, no feature is visible even scanning different regions of the sample at room temperature; all prior STM studies of isolated SCO molecules have been performed at low temperatures,[1,14] so it is possible that the molecules are mobile at higher temperatures. Moreover compound **1** does not have a good anchoring point such as the sulphur atom of the thiocyanates of compound **2**. Though isolated molecules could not be imaged, the lack of features supports the absence of molecular aggregates on the surface: the molecules which are clearly identified by XAS are most likely isolated.

---

[14] a)T. G. Gopakumar, F. Matino, H. Naggert, A. Bannwarth, F. Tuczek, R. Berndt, *Angew. Chem.***2012**, *124*, 6367-6371; *Angew. Chem. Int. Ed.***2012**, *51*, 6262-6266. c) T. Miyamachi, M. Gruber, V. Davesne, M. Bowen, S. Boukari, L. Joly, F. Scheurer, G. Rogez, T. K. Yamada, P. Ohresser, E. Beaurepaire, W. Wulfhekel, *Nature Commun.*, **2012**, *3*, 1-6.

Table S13:Deconvolution results for the submonolayer

Spectra were deconvoluted as a.spectrum(bulk 300 K) + b.spectrum(bulk 100 K) + offset. Baselines, modelled as simple spline manual fits to the spectra before and after the edges,were substracted from reference and experimental spectra before the deconvolution.

This empirical procedure accounts for significant contributions of the NEXAFS oscillations due to the Au substrate, more evident at temperatures under 150 K. Accounting exactly for the Au substrate contribution would have required measurement in the same conditions of a clean substrate. We nevertheless checked the effect of our empirical treatment: without it, HS fractions are systematically increased by 3-4 points of percentage, not changing thus the overall picture. The error values are to be considered consequently underestimated.

T (K)	n_{HS} (%)	n_{LS} (%)	a	b	r^2	Comments
300	69.3(8)	30.7(6)	0.310(2)	0.137(3)	0.981	
100	56.4(10)	43.6(9)	0.253(3)	0.196(4)	0.964	
100	54.6(12)	45.4(12)	0.237(4)	0.197(4)	0.942	
10	60.9(9)	39.1(8)	0.284(3)	0.182(3)	0.973	
10	62.5(9)	37.5(8)	0.285(3)	0.171(3)	0.971	
10	69.0(10)	31.0(8)	0.315(3)	0.141(3)	0.972	laser 658 nm ON for 10 min
10	68.7(9)	31.3(7)	0.305(3)	0.139(3)	0.975	
40	67.7(9)	32.3(8)	0.303(3)	0.145(3)	0.971	
65	55.6(10)	44.4(9)	0.259(4)	0.207(4)	0.962	
100	53.1(9)	46.9(9)	0.246(3)	0.218(4)	0.966	
150	62.5(9)	37.5(8)	0.279(3)	0.168(3)	0.972	
200	69.8(9)	30.2(7)	0.310(3)	0.134(3)	0.976	
300	74.7(9)	25.3(7)	0.326(3)	0.110(3)	0.979	

Below are illustration of the fit results at 300 K, 100 K and 10 K: experimental spectrum (black line), fit (red line), HS (blue line), LS (green line) and baseline+offset (magenta line) components. For clarity this latter curve was added to the fit, HS and LS curves.

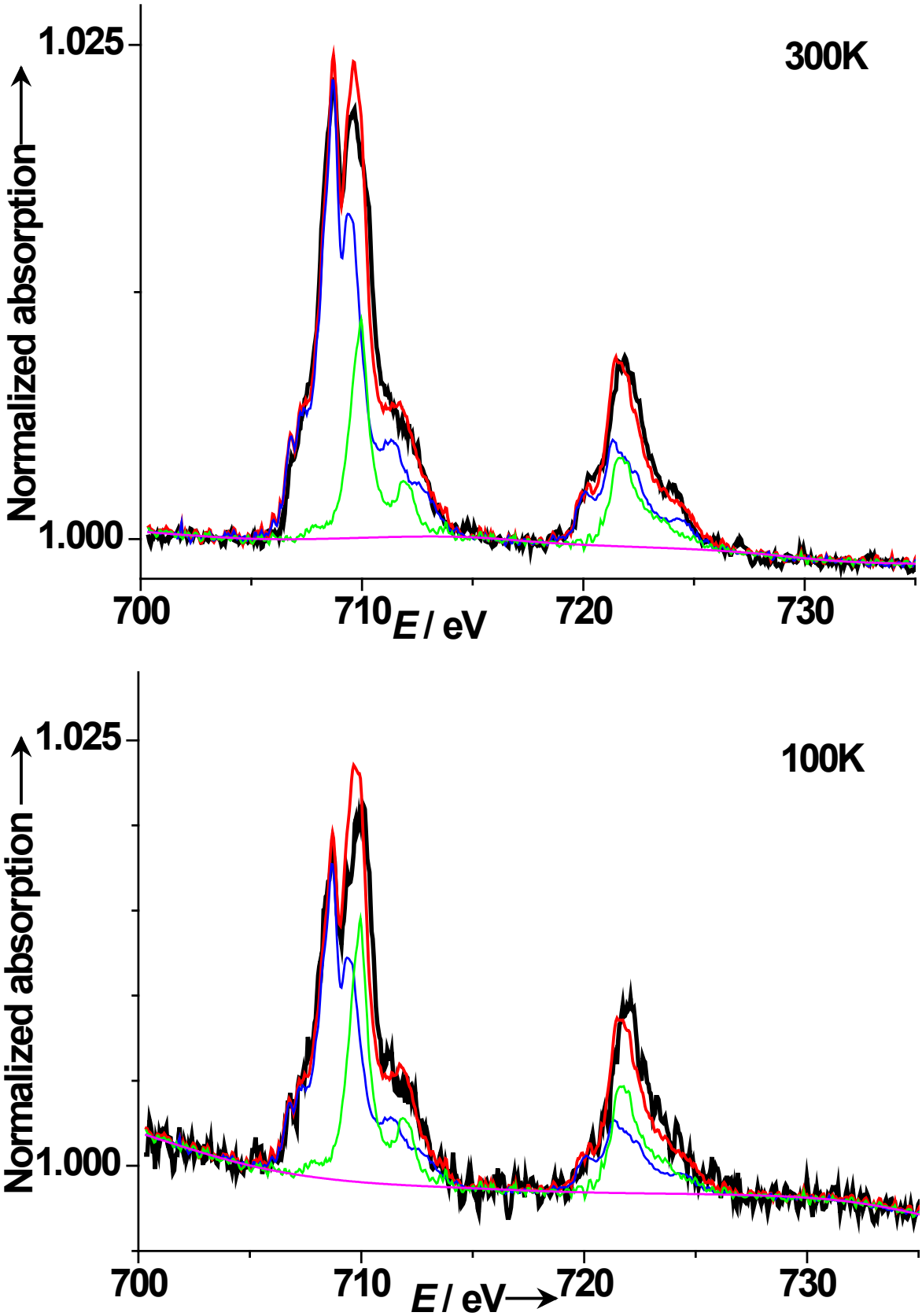
1.025
1.000
Normalized absorption
300K
700
710
720
730
E / eV
1.025
1.000
Normalized absorption
100K
700
710
720
730
E / eV

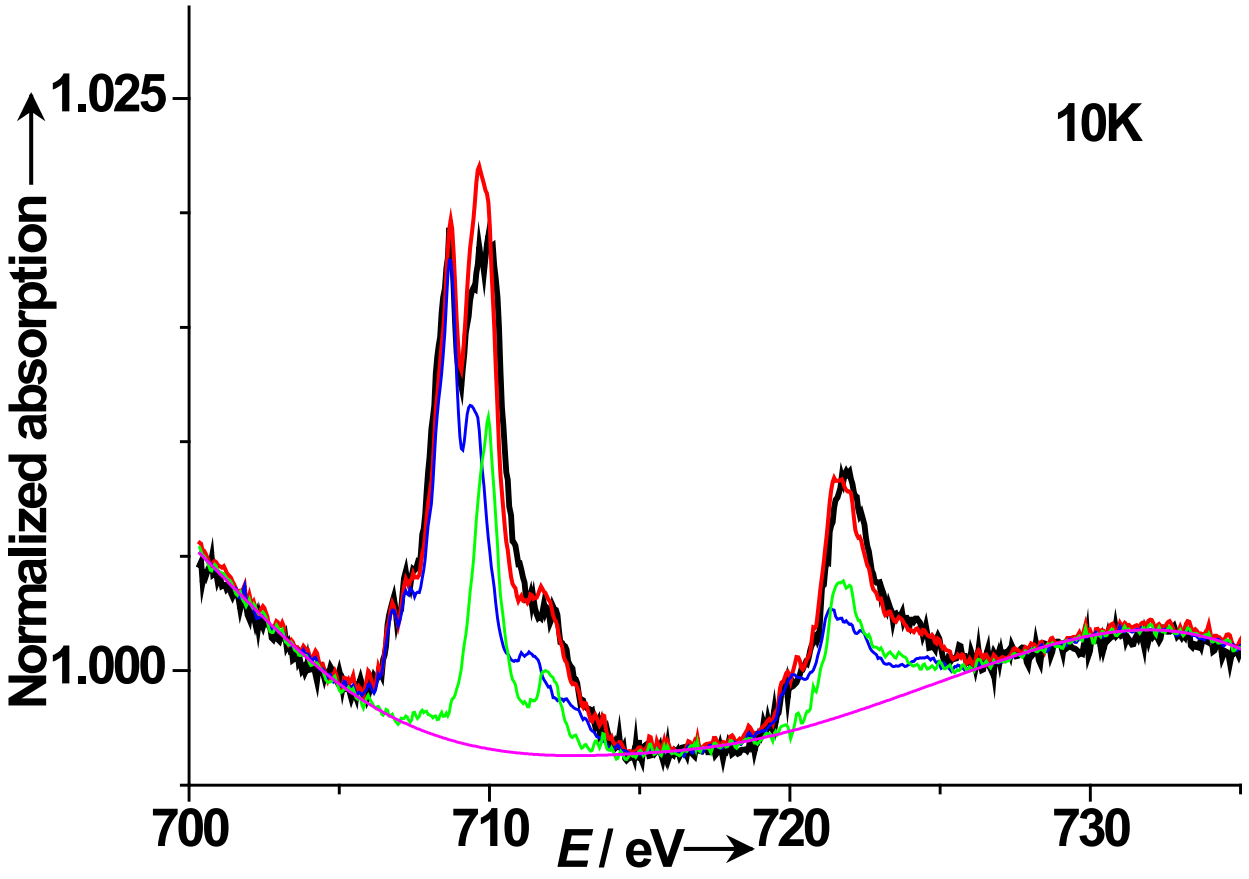
1.025
1.000
Normalized absorption
10K
700
710
720
730
E / eV

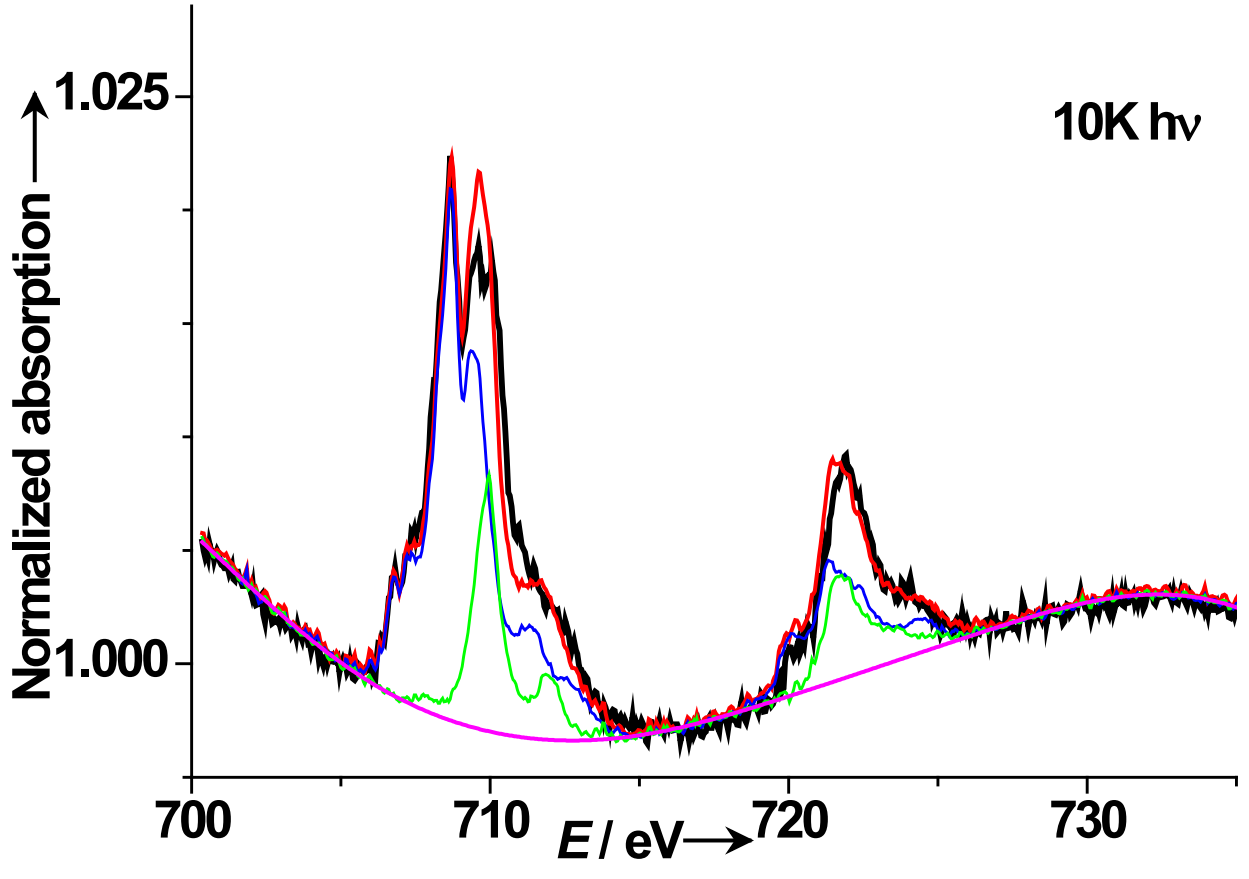
1.025
1.000
Normalized absorption
10K hν
700
710
720
730
E / eV